# Chemolithoautotrophic diazotrophs dominate dark nitrogen fixation in mangrove sediments

Shasha Wang[1#], Lijing Jiang[1#*], Zhuoming Zhao[1], Zhen Chen[1], Jun Wang[1], Karine Alain[3], Liang Cui[1], Yangsheng Zhong[1], Yongyi Peng[1], Qiliang Lai[1], Xiyang Dong[1,2*] and Zongze Shao[1,2*]

[1] Key Laboratory of Marine Genetic Resources, Third Institute of Oceanography, Ministry of Natural Resources of China; State Key Laboratory Breeding Base of Marine Genetic Resources; Fujian Key Laboratory of Marine Genetic Resources; Sino-French Laboratory of Deep-Sea Microbiology (MicrobSea), Xiamen 361005, PR China

[2] Southern Marine Science and Engineering Guangdong Laboratory (Zhuhai), Zhuhai 519000, PR China

[3] Univ Brest, CNRS, Ifremer, EMR6002 BIOMEX, Biologie Interactions et adaptations des Organismes en Milieu EXtrême, IRP 1211 MicrobSea, F-29280 Plouzané, France

# These authors contributed equally to this work.

* Corresponding authors: Zongze Shao, Key Laboratory of Marine Genetic Resources, Third Institute of Oceanography, Ministry of Natural Resources of China, 186 Daxue Road, Fujian 361005, China. Email: shaozz@163.com, Xiyang Dong, Key Laboratory of Marine Genetic Resources, Third Institute of Oceanography, Ministry of Natural Resources of China, 186 Daxue Road, Fujian 361005, China. Email: dongxiyang@tio.org.cn, and Lijing Jiang, Key Laboratory of Marine Genetic Resources, Third Institute of Oceanography, Ministry of Natural Resources of China, 186 Daxue Road, Fujian 361005, China. Email: jianglijing@tio.org.cn

Running title: Chemolithoautotrophic diazotrophs in mangrove sediments

**Abstract**

Diazotrophic microorganisms regulate marine productivity by alleviating nitrogen limitation. So far chemolithoautotrophic bacteria are widely recognized as the principal diazotrophs in oligotrophic marine and terrestrial ecosystems. However, the contribution of chemolithoautotrophs to nitrogen fixation in organic-rich habitats remains unclear. Here, we utilized metagenomic and metatranscriptomic approaches integrated with cultivation assays to investigate the diversity, distribution, and activity of diazotrophs residing in Zhangzhou mangrove sediments. Physicochemical assays show that the studied mangrove sediments are typical carbon-rich, sulfur-rich, nitrogen-limited, and low-redox marine ecosystems. These sediments host a wide phylogenetic variety of nitrogenase genes, including groups I-III and VII-VIII. Unexpectedly diverse chemolithoautotrophic taxa including *Campylobacteria*, *Gammaproteobacteria*, *Zetaproteobacteria*, and *Thermodesulfovibrionia* are the predominant and active nitrogen fixers in the 0-18 cm sediment layer. In contrast, the

18-20 cm layer is dominated by active diazotrophs from the chemolithoautotrophic taxa *Desulfobacterota* and *Halobacteriota*. Further analysis of MAGs show that the main chemolithoautotrophs can fix nitrogen by coupling the oxidation of hydrogen, reduced sulfur, and iron, with the reduction of oxygen, nitrate, and sulfur. Culture experiments further demonstrate that members of chemolithoautotrophic *Campylobacteria* have the nitrogen-fixing capacity driven by hydrogen and sulfur oxidation. Activity measurements confirm that the diazotrophs inhabiting mangrove sediments preferentially drain energy from diverse reduced inorganic compounds other than from organics. Overall, our results suggest that chemolithoautotrophs rather than heterotrophs are dominant nitrogen fixers in mangrove sediments. This study underscores the significance of chemolithoautotrophs in carbon-dominant ecosystems.

**Key words**: Nitrogen fixation; Chemolithoautotroph; *Campylobacterota*; Mangrove sediment; Metagenomic; Metatranscriptomic

## Introduction

Nitrogen serves as an essential component of all living organisms, constituting the main nutrient limiting life on our planet[1,2]. Nitrogen-fixing (diazotrophic) bacteria and archaea convert atmospheric dinitrogen gas ($N_2$) into ammonia ($NH_3$) for assimilation, which is mediated by three types of nitrogenases, including molybdenum-iron nitrogenase Nif (Mo-Fe), vanadium-iron nitrogenase Vnf (V-Fe), and iron-only nitrogenase Anf (Fe-Fe)[3,4]. Biological nitrogen fixation counteracts the removal of bioavailable N by microbial denitrification and anaerobic ammonium oxidation, and provides a source of N to the majority of the biosphere that cannot directly assimilate

$N_2$[5-7]. In particular, marine diazotrophs supply nearly one-half of the global fixed nitrogen demand, and their activity often regulates marine primary productivity[8,9]. However, despite the well-documented ecological and biogeochemical importance of nitrogen fixation in the oceans[2,10,11], due to the high energy demand, only a few bacterial and archaeal populations have been shown to potentially fix nitrogen[12].

In oligotrophic marine environments, chemolithoautotrophs are considered important nitrogen fixers and can enhance the productivity of localized habitats[13]. For example, chemolithoautotrophic sulfur-oxidizing diazotrophs are identified as the key carbon and nitrogen providers to their symbiotic hosts, such as lucinid clams and cold water corals[14-16]. The ability to fix nitrogen has also been demonstrated in deep-sea anaerobic methane-oxidizing archaea from cold seep sediments[17] and methanogenic archaea from hydrothermal vent fluids[18]. In addition, chemolithoautotrophic nitrogen fixation has been well studied in oligotrophic terrestrial environments[13,19]. *Cyanobacteriota* are considered the most important diazotrophs in glaciated forefields[20]. In mine tailings, it is postulated that chemolithoautotrophic diazotrophs utilize reduced sulfur compounds as electron donors for energy production[19]. Additionally, *Beggiatoa*-related chemolithoautrotrophic sulfur-oxidizing bacteria are suggested to actively fix nitrogen in oligotrophic sulfidic caves[14,21]. In contrast, in organic-rich marine ecosystems, nitrogen fixation is often associated with heterotrophs[22-24]. For instance, the process of nitrogen fixation coupled with heterotrophic sulfate reduction has been documented in the sediments of Eckernförde Bay (Baltic Sea) and Narragansett Bay (Rhode Island)[25,26]. Several heterotrophic taxa

within the phyla *Pseudomonadota*, *Chloroflexota*, *Bacteroidota*, *Desulfobacterota*, and *Spirochaetota* are reported as the main diazotrophs in sedimentary ecosystems[27,28]. These previous studies indicate that chemolithoautotrophs are the main nitrogen fixers in oligotrophic environments, whereas biological nitrogen fixation in organic-rich environments is mainly achieved by heterotrophs.

Mangrove sediments are typically considered organic-rich but nitrogen-limited ecosystems[29,30]. Early research revealed a high rate of biological nitrogen-fixing activity mediated by microbes in the surface sediments of mangroves[31-33]. Recent work further indicated that nitrogen fixation rates increased with sediment depth from the surface to 100 cm in mangrove ecosystems[34]. Some heterotrophic prokaryotes in the phyla *Pseudomonadota* (classes *Alpha-* and *Gamma-proteobacteria*), *Desulfobacterota*, *Myxococcota*, and *Bacteroidota* were detected as the prevalent diazotrophs in mangrove sediments on the basis of *nifH* gene amplicons and metagenomics[32,34]. These diazotrophs are thought to depend on reduced organic compounds for their energy and carbon sources[35]. However, more studies have shown that some chemolithoautotrophic bacteria occupy a relative high abundance in mangrove sediment ecosystems[36,37]. For example, members of the genera *Sulfurovum*, *Sulfurimonas*, *Thermodesulfovibrio*, *Desulfobacterium*, and *Desulfococcus* are abundant, with relative abundances > 1% in the sediments (0-20 cm) of Yunxiao mangroves[36]. In other mangrove sediments collected from six locations along the coastline of the BeibuGulf in Guangxi Province, China, chemolithoautotrophic taxa such as *Desulfococcus*, *Nitrosopumilus*, and *Sulfurimonas* are also predominant[38]. The

dominance of chemolithoautotrophs in such organic-rich environments raises the question of whether the nitrogen fixation process is mediated by these autotrophs. Considering that mangrove sediment ecosystems are rich in reduced inorganic compounds such as $H_2$ and sulfide produced by the degradation of organic matter[39,40], we hypothesize that the oxidation of these reduced compounds is another crucial energy pathway for nitrogen fixation.

In this study, to address the roles of chemolithoautotrophic diazotrophs in organic-enriched sediments, we quantified the concentrations of carbon, nitrogen, and sulfur in sediments, carried out activity measurements, and applied metagenomics and metatranscriptomics to investigate nitrogen-fixing microorganisms in mangrove sediments. Furthermore, we inferred the potential metabolic capabilities of the dominant chemolithoautotrophic diazotrophs and confirmed their nitrogen-fixing capacity using culture-dependent methods. Overall, this study reveals the true diazotrophic populations in mangrove surface sediments, and sheds new light on the significant role of chemolithoautotrophs in dark nitrogen fixation within mangrove ecosystems.

## Materials and Methods

### Site description and sampling

The sampling site is located in the mangrove wetland of Jiulong River tributaries in Zhangzhou (117° 45′ N, 24° 20′ E), Fujian Province, China (**Fig. S1**), with a mean annual temperature of 21.2°C and an annual precipitation of 1714.5 mm. The irregular semidiurnal tides were on average 7.70 and -3.03 m of high and low tide levels,

142 respectively. Sediment cores were collected in August 2022 using a 20-cm long PVC
143 sampling column after ebb and sliced at 2-cm intervals into 10 layers (0-2, 2-4, 4-6, 6-
144 8, 8-10, 10-12, 12-14, 14-16, 16-18, and 18-20 cm), yielding a total of 10 samples. At
145 the sampling site, the sediments were not invaded by mangrove roots, and there was
146 no apparent bioturbation. Sediment colors served as an indicator for the presence of
147 active sulfide including the uppermost layer (brownish, sulfide-free), sulfide transition
148 zone (brown to gray), or sulfidic layer (gray or dark, sulfide-rich). Sliced sediments
149 were stored in a portable cooler at 4℃ and transported back to the laboratory within
150 24 h. Each sample was then divided into two subsamples: one was stored at 4℃ for
151 physicochemical properties analysis, and the other was kept at -80℃ for DNA and
152 RNA extraction.

153 **Physicochemical properties analysis**

154 The water content of sediments was measured by drying 10.0 g of fresh sediment at
155 105℃ to a constant weight[34]. The pH and salinity of the sediments were measured in
156 suspensions containing 2.0 g dry sediment in a 1:2.5 (sediment/water) ratio and 1:5
157 (sediment/water) ratio with a pH meter (SevenCompact S220, Mettler Toledo, OH,
158 USA) and a salinity meter (Abbemat 300, Anton Paar, Graz, Austria), respectively[37].
159 Redox potential was measured using a digital voltmeter (Abbemat 550, Anton Paar,
160 Graz, Austria) with Pt and Ag/AgCl reference electrodes[41]. Sediment ammonium
161 ($NH_4^+$), nitrate ($NO_3^-$), and nitrite ($NO_2^-$) were extracted using 2 M KCl, and
162 measured with a continuous flow auto-analyzer (AA3, Bran-Luebbe, Hamburg,
163 Germany)[42]. Porewater sulfate ($SO_4^{2-}$) and thiosulfate ($S_2O_3^{2-}$) concentrations were

164 measured in porewater extracted from 10.0 g of fresh sediment by an ion
165 chromatography (Dionex ICS-1100, Thermo Scientific, MA, USA)[43]. Acid volatile
166 sulfide (AVS) was treated with acid to release $H_2S$ and measured by the iodometric
167 titration method[44]. Sediment samples for measuring the total carbon (TC), total
168 nitrogen (TN), and total sulfur (TS) were dried at 65°C to a constant weight, finely
169 ground, and then measured by a Flash 2000 CHNS/O elemental analyzer (Thermo
170 Scientific, MA, USA)[45]. Total organic carbon (TOC) was measured using the same
171 elemental analyzer after the samples were digested with 5% HCl[19].

172 **DNA extraction and 16S rRNA gene amplicon sequencing**

173 A total of ten sediment samples (5.0 g) were subjected to DNA extraction with a
174 DNeasy PowerMax Soil Kit (12988-10, QIAGEN, Hilden, Germany) according to the
175 manufacturer's protocol. Quality assessment was achieved using a NanoPhotometer
176 spectrophotometer (IMPLEN, CA, USA) and a Qubit 2.0 Fluorometer (Life
177 Technologies, CA, USA). The V3-V4 region of the bacterial 16S rRNA gene was
178 amplified with the universal primers 338F and 806R[46]. Amplicon sequencing was
179 performed on a MiSeq platform (Illumina) using 2 × 300 bp chemistry. Reads were
180 quality controlled using fastp (v0.19.6)[47] and then merged using FLASH (v1.2.11)[48].
181 The amplicon sequence variant (ASV) was obtained after denoising and removal of
182 chimeras by DADA2[49] algorithm recommended by QIIME2[50], and classified using a
183 naive Bayesian classifier in QIIME2 (feature-classifier classify-sklearn) with a
184 confidence score of 0.7 (--p-confidence) against the SILVA v138 database[51].

185 **Quantitative PCR (qPCR) analysis of 16S rRNA gene**

qPCR analyses were performed to estimate the abundance of bacteria and archaea at different depths in the sediment core. PCR reactions were set up using Bio-Rad SsoAdvanced Universal SYBR Green Supermix under the following conditions: 98°C for 2 min, 30 cycles of 98°C for 30 s, 50°C for 30 s, and 72°C for 1 min. Amplification of bacterial and archaeal 16S rRNA genes was performed with the domain-specific primers 338F-806R and 524F10extF-Arch958RmodR, respectively[52]. The specificity of the amplified products was confirmed by melting curve analysis and gel electrophoresis. Standards with known 16S rRNA gene copy numbers were serially diluted from $6.03 \times 10^{10}$ to $6.03 \times 10^{3}$ copies/μL, and the amplification efficiency was between 90 and 105%. The bacterial and archaeal community abundances are shown in **Fig. S2**.

**Metagenomic sequencing, assembly, and binning**

The metagenomic DNA of ten sediment samples was extracted using DNeasy PowerMax Soil Kit as described above. DNA library was prepared with the NEBNext UltraTM DNA Library Prep Kit (E7645, New England Biolabs, MA, USA) following the manufacturer's protocols. The libraries were then measured using an Agilent 5300 Bioanalyzer (Agilent Technologies, CA, USA), and quantification was done using real-time PCR. Sequencing was performed on the HiSeq 2500 platform (Illumina) with 2×150 bp paired-end reads run at Majorbio Biotechnology Co. Ltd., (Shanghai, China). Raw reads were filtered, quality controlled, and trimmed using fastp v0.23.2 with default parameters[47]. All clean reads from different samples were individually assembled with MEGAHIT (v1.1.3)[53] with default settings. Genes were predicted for

CDSs on assembled contigs with Prodigal v2.6.3 with the -p meta option[54]. These sequences were then clustered at 95% amino acid identity using CD-HIT (v4.8.1)[55] with the parameters: -c 0.95 -aS 0.9 -g 1 -d 0, which yielded a total of 6,599,066 non-redundant gene clusters.

Assembled contigs were filtered by length (> 1000 bp) for subsequent binning. Each metagenomic assembly was binned using the metaWRAP v1.3.2 binning module (parameters: -maxbin2 -concoct -metabat2)[56]. All individual assemblies were also concatenated and binned separately using the VAMB tool (v3.0.2; parameters: --minfasta 200000 -o C)[57]. The produced bins from each binning tool were integrated and refined using the Bin_refinement module of metaWRAP (v1.3.2; parameters: -c 50 -x 10). All produced bins were aggregated and dereplicated to a non-redundant set of strain-level metagenome-assembled genomes (MAGs) using dRep v3.4.0 (parameters: -comp 50 -con 10)[58] at 95% average nucleotide identities. Completeness, contamination, and heterogeneity of MAGs were evaluated using CheckM v1.2.1[59]. Additionally, we used GUNC (v1.0.5; default parameters)[60] to assess chimerism and contamination of all diazotrophic MAGs, and MAGpurify software (v2.1.1; default parameters)[61] to check the potential misassigned contigs based on the phylo-markers, clade-markers, tetra-freq, gc-content, and clean-bin modules.

**Taxonomic classification of MAGs**

Taxonomic annotations of each MAG were initially performed using GTDB-Tk v2.4.0 with the "classify_wf" workflow (default parameters) against the reference database (R220)[62]. The assignments were confirmed by the visual inspection of

taxonomic trees. Reference genomes downloaded from NCBI GenBank and MAGs from this study were used to construct a phylogenomic tree based on the concatenation of 43 conserved single-copy genes extracted by CheckM v1.2.1. The maximum-likelihood phylogenomic tree was constructed using IQ-TREE (v2.2.0.3)[63] with the "-m MFP -B 1000" options. All produced phylogenomic trees were visualized using Interactive Tree of Life (iTOL, v5)[64].

**Functional annotation**

For functional profiling of the non-redundant gene catalog, we used the pipeline of Greening lab metabolic marker gene database v.1 with DIAMOND v0.9.14[65,66]. Searches were carried out using all quality-filtered unassembled reads with lengths over 140 bp. These genes were involved in sulfur cycling (*fcc*, *sqr*, *soxB*), nitrogen cycling (*nifH*), carbon fixation (*aclB*, *rbcL*, *acsB*), and NiFe-hydrogenases. Results were filtered based on an identity threshold of 50%, except for NifH and AcsB (65%), and NiFe-hydrogenases (60%)[67]. For individual MAGs and genomes from isolates, gene prediction was performed using Prodigal (v2.6.3, default settings), and the predicted genes were further annotated using KEGG Automatic Annotation Server (KAAS)[68], KEGG-Decoder[69], METABOLIC v4.0101[70], and Rapid Annotation Using Subsystems Technology approach (RAST, v2.0)[71].

**Phylogenetic analyses and conserved residues of functional genes**

For each gene, amino acid sequences from the current study were aligned with reference sequences using MAFFT (v7.490, -auto option)[72], and trimmed using trimAl (v1.2.59, -gappyout option)[73]. Maximum likelihood phylogenetic trees were

constructed using IQ-TREE (v2.2.0.3) with best-fit models and 1000 ultrafast bootstraps. All the tree files were visualized and embellished with iTOL v5. Multiple alignment of NifH, NifD, and NifK superfamily sequences for conserved active site residue analysis was performed using MAFFT (EMBL-EBI)[74] and visualized with Jalview v2.11.2.0[75].

**Abundance profiles**

At the contig level, relative abundances of *nifH* gene in 10 metagenomes were calculated from non-redundant gene catalog using the program Salmon (v1.9.0)[76] in the mapping-based mode (parameters: -validate Mappings -meta). Genes per million (GPM) values were used as a proxy for gene abundance, as described elsewhere[77]. GPM value was normalized based on the gene length and sequencing depth[78]. At the genome level, the relative abundance of each *nif*-containing MAG was profiled by mapping quality-trimmed reads from the 10 metagenomes against the MAGs using CoverM v1.2.1 in genome mode (parameters: -m relative_abundance --trim-min 0.10 --trim-max 0.90 --min-read-percent-identity 0.95 --min-read-aligned-percent 0.75 --min-covered-fraction 0)[79].

**Metatranscriptomic analysis**

Total RNA was extracted from the same samples used for metagenome analysis using the RNeasy PowerSoil Total RNA Kit (12866-25, QIAGEN, Hilden, Germany) according to the manufacturer's protocol. RNA purity and concentration were evaluated using a Qubit 2.0 Fluorometer (Life Technologies, CA, USA). RNA integrity was determined using an Agilent 5300 Bioanalyzer (Agilent Technologies,

CA, USA). Whole transcriptome amplification of total RNA was carried out using the RNA REPLI-g Cell WGA & WTA Kit (150054c, QIAGEN, Hilden, Germany) according to the manufacturer's protocol. To enrich messenger RNA (mRNA), ribosomal RNA was depleted from total RNA using the RiboCop rRNA Depletion Kit (Lexogen, Vienna, Austria). Whole mRNA-Seq libraries were generated by Majorbio Biotechnology Co. Ltd., (Shanghai, China) using the NEBNext Ultra Nondirectional RNA Library Prep Kit (E6111, New England Biolabs, MA, USA) following the manufacturer's instructions. The constructed libraries were sequenced on a NovaSeq 6000 platform (Illumina), and 150 bp paired-end reads were generated.

Raw metatranscriptomic reads were quality filtered in the same manner as metagenomes. The reads corresponding to ribosomal RNAs were removed using SortMeRNA v.4.3.4[80] with default parameters with the smr_v4.3_default_db database. Subsequently, these high-quality metatranscriptomic reads were mapped to predicted protein-coding genes from the reference gene catalog and *nifH*-containing MAGs using Salmon v.1.9.0[76] in mapping-based mode (parameters: -validate Mappings -meta), with mapping rates of 7.11-14.87% and 0.02-0.67%, respectively. The expression level of each gene was normalized to transcripts per million (TPM) based on gene length and sequencing depth.

**Pure culture isolation and growth characteristics**

Sediment samples were collected in January 2019 from a mangrove wetland in Zhangzhou as described above. For isolation, 1.0 g sediment samples were transferred into 50 ml serum bottles containing 10 ml MMJS medium with a gas phase mixture of

296 80% $N_2$/18% $CO_2$/2% $O_2$ (200 kPa), and incubated at 28°C as previously described[81].
297 Cells were purified via the dilution-to-extinction technique using the same medium.
298 The purity of the culture was confirmed by microscopic examination and 16S rRNA
299 gene sequencing. Genomic DNA of pure cultures was extracted using the method
300 described by Jiang *et al*. (2009)[82] and sequenced by Majorbio Biotechnology Co. Ltd.,
301 (Shanghai, China) using a HiSeq 4000 platform (Illumina, San Diego, CA, USA).
302 Heterotrophic growth was tested in a MMJS medium without $NaHCO_3$ with a
303 series of organic compounds as the sole carbon source under a gas phase of 76%
304 $N_2$/20% $CO_2$/4% $O_2$ (200 kPa)[83]. These organic carbon sources included: 0.1% (w/v)
305 peptone, yeast extract, tryptone, starch, casein, and casamino acids, 5 mM of acetate,
306 formate, citrate, tartrate, succinate, propionate, and pyruvate, 5 mM each of 20 amino
307 acids, 0.02% (w/v) sucrose, galactose, glucose, lactose, fructose, maltose, and
308 trehalose. The utilization of these organic compounds as alternative energy sources
309 was also examined in MMJ medium in the absence of thiosulfate under a gas phase of
310 76% $N_2$/20% $CO_2$/4% $O_2$ (200 kPa). Additionally, to examine the utilization of
311 inorganic and organic nitrogen sources, ammonium chloride (1 mM), sodium nitrate
312 (1 mM), sodium nitrite (1 mM), urea (1 mM), or a mixture of 20 amino acids (1 mM)
313 was added to MMJHS medium lacking all nitrogen sources under a gas phase of 76%
314 $H_2$/20% $CO_2$/4% $O_2$ (200 kPa).
315 **Characterization of $N_2$ fixation in mangrove sediment samples and isolates**
316 An acetylene reduction assay with slight modifications was used to measure
317 nitrogenase activity[84,85]. Approximately 1.0 g sediment samples with four layers (0-2,

6-8, 12-14, and 16-18 cm) were separately mixed with 10 mL autoclaved MMJ medium in a 60 mL serum bottle with 10% (v/v) acetylene added to the headspace. Autotrophic $N_2$-fixing potential was tested with 10 mM $Na_2S_2O_3$ as the energy source and 10 mM $NaHCO_3$ as the carbon source under 70% $H_2$/20% $CO_2$ (200 kPa). For heterotrophic diazotrophic potential, 10 mM sucrose was supplied as the carbon and energy sources. A blank control treatment was set up by adding only sediments. For the 0-2 cm layer, microoxic condition was set with 4% $O_2$ as the sole electron acceptor during incubation. For the other three layers, $S^0$ (5 g $L^{-1}$) was added for anoxic condition, and sulfide was produced with a smell like rotten eggs. Samples were incubated at 30°C and 180 rpm in the dark. A 7890B GC-FID (Agilent Technologies, CA, USA) equipped with an Al/KCl capillary column (Agilent Technologies, CA, USA) was used to monitor the production of ethylene in the headspace.

The $^{15}N$ activity of the sediments and isolates was determined using the $^{15}N_2$ assimilation method with slight modifications (eg, time and volume)[19]. The culture conditions and treatment sets were established as described above. All cultures were incubated at 30°C in the dark and analyzed on day 10 for sediments and day 1 for isolates. All samples including sediments and isolates were then harvested by centrifugation (10,000 x g, 4°C, 20 min) after turbidity became apparent, washed twice in cold 20 mM Tris buffer in artificial sea water, and freeze dried overnight[86]. The atomic % $^{15}N$ of freeze-dried cells was determined using a Carlo-Erba elemental analyzer (Model NA 1500, Fisons Instruments, MA, USA) linked to a Finnegan MAT (ThermoQuest, CA, USA) Delta S isotope ratio mass spectrometer[22].

## Results and discussion

### Physicochemical characteristics of mangrove sediments

We measured total carbon (TC), total organic carbon (TOC), total nitrogen (TN), $NO_3^-$, $NO_2^-$, $NH_4^+$, total sulfur (TS), acid volatile sulfide (AVS), $SO_4^{2-}$, redox potential, moisture, pH, and salinity to characterize their vertical distributions from 0 to 20 cm depth in Zhangzhou mangrove sediments (**Fig. S3**). High concentrations of TC and TOC (2.41-2.59% and 2.10-2.35%, respectively) were observed at all depths, whereas TN concentrations were low, ranging from 0.12-0.14% (**Fig. S3 A-C**). The C/N ratio ranged from 18.39 to 21.97 in the 0-20 cm layer, which is similar to that in other mangrove sediment ecosystems, and distinct from that in other habitats, such as tidal flats, brackish water, and freshwater[87,88]. The concentrations of inorganic nitrogen, including $NO_3^-$ (0.14-0.65 mg/kg) and $NO_2^-$ (0.01-0.04 mg/kg), were low and decreased consistently with depth (**Fig. S3 D, E**). $NH_4^+$ concentrations varied between 1.27 and 3.23 mg/kg at all sediment depths (**Fig. S3 F**). Similar low ammonium-N concentrations have been reported in other mangrove habitats[34,36,89], underscoring the nitrogen limitation in Zhangzhou mangrove surface sediments.

High concentrations of TS and AVS increased with sediment depth, peaking in the 18-20 cm layer (**Fig. S3 G, H**), whereas the $SO_4^{2-}$ concentration exhibited a decreasing trend, with the highest concentration in the upper 0-6 cm layer (**Fig. S3 I**). Traces of thiosulfate ($S_2O_3^{2-}$) were detected only in surface sediments (~40 μM and ~20 μM in the 0-2 cm and 2-4 cm layers, respectively). The redox potential (Eh) of the top 0-2 and 2-4 cm layers was 320 and 252 mV, respectively, and this value

362 decreased sharply with depth below 4 cm, reaching the lowest value of -120 mV at the
363 deepest layer (**Fig. S3 J**). Among all measured parameters, TN, $NO_3^-$, $NO_2^-$, and
364 $SO_4^{2-}$ were negatively correlated with depth ($P < 0.05$), whereas TS and AVS showed
365 a positive correlation ($P < 0.05$) (**Fig. S4**). Collectively, these findings highlight that
366 Zhangzhou mangrove surface sediments are characterized by a carbon and nitrogen
367 imbalance coupled with a richness of reduced sulfur compounds.

368 **Diversity, distribution and activity of nitrogen-fixing genes across sediment**
369 **depths**

370 The *nifH* gene, encoding an essential nitrogenase enzyme protein, is commonly used
371 to investigate the diversity and prevalence of diazotrophs across diverse settings[90,91].
372 Annotations of contigs assembled from the 10 metagenomes extracted from the
373 mangrove sediment samples revealed a total of 154 non-redundant *nifH* homologs
374 falling into the nitrogenase superfamily (**Fig. 1A; Table S1**). Except for nitrogenase-
375 like groups of IV to VI[92], these homologs were classified into canonical nitrogenase
376 sequences (groups I-III)[93] and two newly proposed lineages, groups VII and VIII[10]
377 (**Fig. 1A**). Two novel lineages are also considered to be bona fide *nifH* based on the
378 analyses of nitrogenase conserved motifs, as detailed below. These results indicate
379 that the mangrove sediments host more diverse nitrogenase genes than previously
380 thought[34].

381 The abundances of *nifH* gene ranged from 20.1 to 34.1 genes per million (GPM)
382 from the surface to 18 cm, peaking at 47.8 GPM in the 18-20 cm layer (**Fig. 1B**). At
383 the phylum level, the most abundant putative diazotrophs in the mangrove sediments

were *Desulfobacterota*, *Pseudomonadota*, and *Campylobacterota* (**Fig. 1B**). At the class level, *Gammaproteobacteria*, *Campylobacteria*, and *Desulfobacteria* were the most prevalent (**Fig. S5A**). Despite the absence of transcripts in the 14-16 cm layer, *nifH* transcripts were detected throughout the other layers, indicating that nitrogen-fixing activity is present at most sediment depths (**Fig. 1C**). At the four layers with high *nifH* transcripts, *Campylobacterota*, *Nitrospirota*, and *Pseudomonadota* emerged as the potential predominant nitrogen-fixing groups (**Fig. 1C**). Specifically, there was a niche differentiation among these groups. In the 6-8 and 10-12 cm layers, *nifH* transcripts values were mainly affiliated with the members of the class *Campylobacteria* (**Fig. S5B**), and in the 12-14 cm layer, *nifH* transcripts were highly expressed in the class *Thermodesulfovibrionia*. In the 16-18 cm layer, higher *nifH* transcripts values were found from the classes *Gammaproteobacteria* and *Campylobacteria* (**Fig. S5B**).

Considering the dominant and transcriptionally active diazotrophs were mainly belonged to the chemolithoautotrophic *Campylobacterota* and *Nitrospirota*, further exploration was conducted to determine the correlation between *nifH* and carbon fixation genes (eg, *aclB*, *rbcL*, and *acsB*), sulfur oxidation genes (eg, *sqr* and *soxB*) or hydrogen oxidation gene (*hydB*) within mangrove sediments. The results revealed strong and significant correlations between the transcriptional activity of *nifH* and the aforementioned genes (**Fig. S6**), suggesting a robust link between diazotrophic and putative chemolithoautotrophic populations in mangrove sediments. Therefore, it is assumed that these chemolithoautotrophic microorganisms may constitute key active

groups for *in situ* nitrogen fixation in mangrove sediments.

**Potential nitrogen-fixing microorganisms identified within mangrove sediments**

Through metagenomic assembly and binning strategies, we recovered 180 bacterial (*n*=172) and archaeal (*n*=8) population genomes with > 50% completeness and < 10% contamination, which belonged to 24 phyla based on the GTDB taxonomy (**Table S2**). Among these genomes, 36 MAGs (33 bacterial and 3 archaeal MAGs) spanning twelve phyla were identified as potential nitrogen-fixing microorganisms, including *Desulfobacterota* (*n*=10), *Pseudomonadota* (*n*=6), *Campylobacterota* (*n*=4), *Chloroflexota* (*n*=3), *Halobacteriota* (*n*=3), *Myxococcota* (*n*=3), *Bacteroidota* (*n*=2), *Methylomirabilota* (*n*=1), *Nitrospirota* (*n*=1), *Spirochaetota* (*n*=1), *Schekmanbacteria* (*n*=1), and SZUA-182 (*n*=1) (**Fig. 2A; Table S3**). Subsequent phylogenetic analyses revealed that nitrogenases from these 36 MAGs were categorized into groups I, II, VII, and VIII (**Fig. 2B**), and all of which were observed to have conserved active sites among NifH, NifD, and NifK (**Fig. S7-9**). Furthermore, NifH sequences from the same taxonomic group did not cluster into a single clade (**Fig. 2A, B**), which may be explained by horizontal gene transfer (HGT)[94,95].

Among 36 potential nitrogen-fixing MAGs, a majority (21/36) encoded carbon fixation pathways, with at least 60% of the genes and all the key enzymes[96] (**Fig. 2B; S10**). The reductive citric acid (rTCA) cycle was encoded by the class *Campylobacteria* (*n*=2) of the phylum *Campylobacterota* (**Fig. 2B; S11**). The Calvin-Benson-Bassham (CBB) cycle was encoded by five *Pseudomonadota* MAGs including the classes *Gammaproteobacteria* (*n*=4) and *Zetaproteobacteria* (*n*=1), and

three *Halobacteriota* MAGs including the classes *Methanosarcinia* (*n*=2) and *Methanomicrobia* (*n*=1) (**Fig. 2B; S12**). The Wood-Ljungdahl (WL) pathway was encoded by eight *Desulfobacterota* MAGs including the classes *Desulfobacteria* (*n*=6) and *Desulfobulbia* (*n*=2), one *Myxococcota* MAG including the class *Polyangia* (*n*=1), one *Nitrospirota* MAG including the class *Thermodesulfovibrionia* (*n*=1), and one *Halobacteriota* MAG including the class *Methanosarcinia* (*n*=1) (**Fig. 2B; S13**). These findings suggest that the microorganisms represented by these MAGs could be potential chemolithoautotrophic diazotrophs.

Read mapping of the 36 diazotrophs showed that they were widely distributed at different sediment depths (**Fig. 3A; Table S4**). When considered individually, the chemolithoautotrophic taxon *Campylobacterota* was the most abundant at most sediment depths except 18-20 cm layer (**Fig. 3A**), indicating its important role as a potential nitrogen fixer in mangrove sediments. A previous study indicated that *Campylobacteria* was abundant in the surface (0-15 cm) mangrove sediments, coupling sulfur oxidation and denitrification processes[36]. Furthermore, *Pseudomonadota* and chemolithoautotrophic *Nitrospirota* also exhibited higher abundances in the 0-18 cm layer, but demonstrated a consistent decrease in abundance with sediment depth (**Fig. 3A**). Whereas in the 18-20 cm layer, members of the phyla *Desulfobacterota*, *Myxococcota*, and *Halobacteriota* were the most predominant diazotrophs (**Fig. 3A**). The high abundances could point to an important role for these phyla in nitrogen fixation in deeper sediments. A recent study indicated that in deeper mangrove sediments around 30 cm, members from *Desulfobacterota* and

*Halobacteriota* were dominant[37]. At the class level, *Campylobacteria*, followed by several other classes including *Desulfobacteria*, *Gammaproteobacteria*, *Dehalococcoidia*, and *Thermodesulfovibrionia*, were notably predominant in the 0-18 cm layer, whereas in the 18-20 cm layer, the classes such as *Desulfobacteria*, YA12-FULL-58-9, and *Methanomicrobia* were the most abundant (**Fig. S14A**). Therefore, chemolithoautotrophic organisms consistently emerge as the dominant nitrogen fixers in the top 0-20 cm of mangrove sediments.

To evaluate the *in situ* expression of these diazotrophs, ten metatranscriptomes from different sediment depths were mapped against MAGs encoding nitrogenase (**Table S5**). The results showed that *nifH* gene transcripts in the 0-18 cm layer were predominantly expressed in ten chemolithoautotrophic MAGs from the phyla *Campylobacterota* (*n*=4), *Pseudomonadota* (*n*=5), and *Nitrospirota* (*n*=1) (**Fig. 3B**), suggesting that they could be the primary nitrogen fixers in mangrove sediments. At the class level, the *nifH* genes of *Campylobacteria* were transcribed from low to high levels in several layers, up to 1456.38 transcripts per million reads (TPM), and the transcript values from *Thermodesulfovibrionia* in the 6-8 and 12-14 cm layers were 412.15 and 1122.25 TPM, respectively (**Fig. S14B**). Furthermore, *nifH* transcripts were expressed in the class *Gammaproteobacteria* in multiple sediment layers with higher levels in the surface layers (0-6 cm), whereas this transcription was found in *Zetaproteobacteria* in the 10-12 cm and 16-18 cm layers, with 135.17 and 41.94 TPM, respectively (**Fig. S14B**). This study is the first report indicating that *Zetaproteobacteria* and *Thermodesulfovibrionia* can actively fix nitrogen, implying

that they may play important roles in the nitrogen cycle in addition to their previously reported roles[96,97]. In the deepest layer (18-20 cm), the *nifH* transcripts were mainly expressed in the phyla *Desulfobacterota* and *Halobacteriota,* but with lower values of 10.05-30.82 and 30.30 TPM, respectively (**Fig. 3B**), indicating that these taxa may play elevated roles in nitrogen fixation in deeper layers. Interestingly, no *nifH* transcripts from previously reported heterotrophic diazotrophs[52,98-99], such as certain MAGs from the phyla *Myxococcota* (*n*=2), *Bacteroidota* (*n*=2), or *Spirochaetota* (*n*=1), were expressed (**Fig. 3B**). Overall, our results further confirm that chemolithoautotrophs dominate dark nitrogen fixation in mangrove sediments.

**Energy production pathways of dominant chemolithoautotrophic diazotrophs**

To predict the functional capabilities of dominant chemolithoautotrophic diazotrophs, the metabolic potentials of MAGs were determined based on marker genes and pathways (**Fig. 4A; Table S6-8**). For sulfur metabolism, all *Campylobacterota* MAGs (D5_bin.8, D8_bin.38, D8_bin.28, and D10_bin.20) harbored multiple copies of genes encoding sulfide:quinone oxidoreductase (Sqr) (**Fig. 4A; S15**), which catalyzes the oxidation of sulfide to elemental sulfur[100]. A nearly complete Sox system (SoxACDXYZ) was identified in D10_bin.20, indicating that it has the genetic potential to oxidize thiosulfate[101]. D5_bin.8 and D8_bin.28 contained partial Sox systems (**Fig. 4A; S16**), potentially due to the low MAG completeness. Moreover, D5_bin.8 and D10_bin.20 contained genes encoding sulfite dehydrogenase (SorAB), indicating that they can oxidize sulfite to sulfate[101]. For hydrogen metabolism, all four MAGs contained Group 1 [NiFe]-hydrogenases (Hyd and Hya), and only D10_bin.20

494 contained Group 2 [NiFe]-hydrogenases (Hup) (**Fig. 4A; S17**), which may endow
495 them the potential to use hydrogen as an energy source[102]. Regarding electron
496 acceptors, D5_bin.8, D8_bin.38, and D10_bin.20 contained oxygen-utilizing genes
497 encoding *cbb3*-type cytochrome c oxidases (CcoNOPQ) and *caa3*-type cytochrome c
498 oxidases (CoxAB) (**Fig. 4A**). In comparison with the low-oxygen-affinity *caa3*-type
499 oxidase induced under oxic conditions, *cbb3*-type oxidase is a high-affinity terminal
500 oxygen reductase capable of functioning under microoxic to anoxic conditions[103,104].
501 The presence of cytochromes could also function as residual $O_2$ scavengers for the
502 detoxification of $O_2$/reactive oxygen species (ROS) to protect $O_2$-sensitive
503 proteins[105,106]. Additionally, polysulfide reductase (Psr), which is involved in
504 elemental sulfur reduction, was encoded by four MAGs, indicating their potential
505 ability to perform sulfur reduction under anoxic conditions[100]. These results show that
506 these *Campylobacteria* can use reduced sulfur compounds and hydrogen as electron
507 donors, and oxygen and elemental sulfur as terminal electron acceptors to generate
508 ATP for nitrogen fixation.

509 Within the phylum *Pseudomonadota*, four MAGs (D5_bin.11, D6_bin.23,
510 D9_bin.7, D10_bin.17) belonged to the class *Gammaproteobacteria*, and one MAG
511 (D4_bin.11) belonged to the class *Zetaproteobacteria* (**Table S3**). For sulfur
512 metabolism, all MAGs harbored different copies of *sqr* for sulfide oxidation and
513 lacked SorAB for sulfite oxidation (**Fig. 4B; S15**). D5_bin.11 and D10_bin.17
514 encoded an incomplete Sox system (SoxABXYZ), and D6_bin.23 only contained the
515 subunits of SoxAXYZ (**Fig. 4B; S16**). For hydrogen metabolism, all MAGs encoded

Group 1 [NiFe]-hydrogenase (Hdy and/or Hya) and lacked Group 2 [NiFe]-hydrogenase (Hup) (**Fig. 4B; S17**). The gene encoding cytochrome *c*-porin (Cyc2), which is involved in iron oxidation, was found in D4_bin.11. *Zetaproteobacteria* are known to be obligate chemolithoautotrophic iron-oxidizing bacteria that oxidize Fe at a circumneutral pH[97]. With respect to electron acceptors, D5_bin.11, D6_bin.23, and D10_bin.17 contained the genes encoding CcoNOPQ, CoxAB, and a cytochrome *bd* ubiquinol oxidase (CydAB) for oxygen respiration, which has a high affinity for oxygen and allows growth under microoxic conditions[102]. D9_bin.7 encoded genes for CcoNOPQ and CydA, and D4_bin.11 encoded genes for CcoNOPQ and CoxAB. Furthermore, D6_bin.23 and D10_bin.17 contained NapAB for nitrate reduction to nitrite, and only NorBC and NosZ were found in D5_bin.11 (**Fig. 4B**). Furthermore, Psr involved in elemental sulfur reduction was encoded by most *Gammaproteobacteria* MAGs. These results show that *Gammaproteobacteria* and *Zetaproteobacteria* can use sulfide, thiosulfate, iron, or hydrogen as electron donors, and oxygen, nitrate, and elemental sulfur as terminal electron acceptors to generate ATP for nitrogen fixation.

One MAG (D4_bin.8) belonged to the class *Thermodesulfovibrionia* from the phylum *Nitrospirota* (**Table S4**). For sulfur metabolism, D4_bin.8 lacked all genes encoding sulfur oxidation such as Sqr, Sox, and Sor (**Fig. 4C**). Furthermore, D4_bin.8 encoded Group 1 [NiFe]-hydrogenase (Hyd and Hya) and NAD-reducing hydrogenase (HoxHYU) for hydrogen oxidation (**Fig. 4C; S17**). With respect to electron acceptors, D4_bin.8 contained all genes encoding the sulfate reduction

pathway, including dissimilatory sulfite reductase (DsrABC) and adenylylsulfate reductase (AprAB) (**Fig. 4C**). D4_bin.8 also contained the enzymes CcoNOPQ and CoxAB for oxygen respiration and NapAB for nitrate reduction to nitrite. The Psr for elemental sulfur reduction was absent in D4_bin.8. These results show that *Thermodesulfovibrionia* can couple hydrogen oxidation with sulfate reduction, denitrification, or aerobic respiration to obtain energy for nitrogen fixation, which is in agreement with other studies of this class[96,107,108].

**Isolation of potential dominant diazotrophs from chemolithoautotrophic *Campylobacterota***

Ten strains named HSL-C5, HSL1-2, HSL1-6, HSL3-1, HSL3-2, HSL3-7, HSL-3221, HSL-1716, HSL-1656, and HSL1-3 were successfully isolated from mangrove sediments (**Fig. 5A**). They shared the highest 16S rRNA gene sequence similarities with members from the genera *Sulfurimonas* and *Sulfurovum* of the phylum *Campylobacterota* (**Table S9**), which were two predominance genera in *in situ* mangrove sediments by 16S rRNA gene from metagenomics and amplicon sequencing (**Fig. S18; S19**). Furthermore, phylogenetic tree based on the 16S rRNA gene sequences of ASVs from the two genera and our isolates showed that strain HSL1-3 was most closely related to the two most predominant members represented by ASV7 (up to 6.07% relative abundance) and ASV18 (up to 2.07% abundance) from the genus *Sulfurovum*, with 97.14% and 97.03% sequence identity, respectively (**Fig. 5A; Table S10**). Strain HSL3-7 formed a cluster with the most dominant ASV3 (up to 2.46% abundance) from the genus *Sulfurimonas* with 99.03% sequence

identity. Strain HSL-3221 corresponded to the second most predominant ASV19 (up to 1.04% abundance) of the genus *Sulfurimonas* with 98.51% sequence identity (**Fig. 5A; Table S10**). Thus, these isolates represented the predominant members of the genera *Sulfurimonas* and *Sulfurovum* in *in situ* mangrove sediments. Additionally, upon evaluating average amino acid identity (AAI)[109] and performing a genome-based phylogenomic analysis[110], these ten strains were assigned to five genera including three potentially new genera in the family *Sulfurimonadaceae* (**Fig. S20; S21**).

All ten isolates harbored a complete nitrogen fixation gene cluster encoding the nitrogenase designated NifHDKENB (**Fig. 5B**). Gene neighborhood analyses of these strains revealed that electron transfer proteins, regulatory proteins, and those necessary for nitrogenase cofactor biosynthesis were encoded among the *nif* gene clusters (**Fig. 5B**), which was also found in previous reports[15,111]. Furthermore, physiological characterization revealed that all ten isolates were obligate chemolithoautotrophs, and none of the organic compounds tested supported their growth as carbon and energy sources. Genes involved in the oxidation of sulfur and hydrogen and the reduction of various terminal acceptors in these ten isolates are shown in **Table S11,** which could supply energy for nitrogen fixation. Indeed, nitrogen fixation is not common in chemolithoautotrophic *Campylobacterota* and so far only described for the member of *Sulfuricurvum kujiense* isolated from underground crude oil storage[112]. Thus, *Campylobacterota* strains containing nitrogenase genes identified herein may possess a competitive advantage in nitrogen-limited mangrove sediments. Compared with heterotrophic nitrogen-fixing

582 bacteria[28,113], fewer chemolithoautotrophic diazotrophs have been cultured by far.
583 Prior to our study, only several bacteria belonging to the phyla *Pseudomonadota* and
584 *Aquificota* have been isolated from freshwater, mine wastes, salt marshes, and hot
585 springs, which could grow chemolithoautotrophicly using reduced sulfur compounds,
586 hydrogen, As, or Sb as an energy source to fix $N_2$[19, 114-117].

587 **Nitrogen fixation activity in the isolates and mangrove sediments**

588 The seven active strains that exhibited robust growth were selected to determine their
589 ability to fix $^{15}N_2$ intracellularly using the $^{15}N$-labeled isotope analyses. The results
590 showed that these seven strains were capable of fixing $^{15}N_2$ with $N_2$ as the sole
591 nitrogen source under a gas mixture of $^{15}N_2$:$CO_2$ (**Fig. 6A, B**). As a comparison,
592 strains *Sulfurimonas hydrogeniphila* NW10$^T$ and *Sulfurovum indium* ST-419$^T$, which
593 lacked nitrogen fixation gene clusters, could not perform nitrogen fixation. As for the
594 energy sources, hydrogen and sulfur compounds such as thiosulfate and elemental
595 sulfur could be utilized with hydrogen as a preferred energy source, when these
596 strains utilize oxygen, thiosulfate (only strain HSL1-3), or elemental sulfur as the sole
597 electron acceptor (**Fig. 6A, B**). Nitrogen fixation is linked to hydrogen formation[118].
598 Hence, the recovery of energy via hydrogen oxidation could minimize the energy
599 losses during nitrogen fixation. Combining N fixation with hydrogen oxidation to save
600 energy has been described for *Cyanobacteriota* but has also been mentioned for other
601 members of the phylum *Pseudomonadota* such as the genera *Thermochromatium* and
602 *Rhodospirillum*[119,120]. Furthermore, $^{15}N_2$ fixation was completely inhibited by the
603 addition of ammonia at both low and high concentrations (1 mM and 40 mM $NH_4Cl$),

and inhibited to some extent by the addition of 1 mM $NaNO_3$ and $NaNO_2$ in all seven strains (**Fig. S22**). In contrast, organic nitrogen compounds such as urea and amino acids did not inhibit their nitrogen fixation activity (**Fig. S22**), which is attributed to these isolates not being able to grow on these compounds as nitrogen sources. Additionally, these seven strains were able to fix $^{15}N_2$ at both low and high oxygen concentrations (4% and 20% $O_2$), which may be due to their antioxidant systems[121,122].

To verify the contribution of chemolithoautotrophs to nitrogen fixation in mangrove sediments, we carried out activity measurements by acetylene reduction assay and $^{15}N_2$ incorporation assay (**Fig.6 C, D**). Based on the measured redox potential and the highest transcript expression detected in this study, four sediment layers (0-2, 6-8, 12-14, and 16-18 cm) were chosen to examine the nitrogen-fixing activity. The results showed that the autotrophic diazotrophic activities ranged from $0.52 \pm 0.07$ to $0.79 \pm 0.06$ nmol $g^{-1}$ $day^{-1}$, which were significantly higher than the heterotrophic diazotrophic activities ($0.28 \pm 0.04$ to $0.46 \pm 0.08$ nmol $g^{-1}$ $day^{-1}$) in mangrove sediment samples under both microoxic and anoxic conditions (**Fig. 6C**). Without supplementation of any carbon or energy source, the nitrogenase activity of the original sediments was merely $0.19 \pm 0.04$ to $0.34 \pm 0.04$ nmol $g^{-1}$ $day^{-1}$ (**Fig. 6C**). In addition, the $\delta^{15}N$ values were significantly higher in the cultures amended with inorganic carbon and energy sources than in the treatments with organics or in the original sediments after 10 days of incubation (**Fig. 6D**).

**Implications for chemolithoautotrophic diazotrophy in mangrove sediments**

626 Taken together, our findings imply that chemolithoautotrophic diazotrophy rather than
627 heterotrophic diazotrophy dominates in organic-rich and nitrogen-limited mangrove
628 sediment habitats, which may be attributed to the low redox potential and abundant
629 reduced inorganic compounds such as $H_2$ and $H_2S$ in these setting. Generally, in
630 marine sediments, when Eh < 0 mV, the sediment is strongly reductive, and when the
631 Eh values range from 0 to 200 mV, the sediment is slightly reductive[123,124]. In our
632 study, sediments below 4 cm exhibited highly reduced conditions with Eh < 0 mV
633 (**Fig. S3 J**). The negative redox potential in deeper sediments except surface
634 sediments indicates that the mangrove sediments are mostly water-logged without
635 much periodical aeration, which is consistent with the microbiological data.
636 Moreover, aerobic microorganisms consume oxygen during the decomposition of
637 organic matter[125], which also leads to oxygen depletion with depth increase. However,
638 considering the interference of mangrove root extension and the burrowing activity of
639 polychaetes and crabs[126], the redox gradients in anoxic sediments may be dynamic.
640 Besides the low redox potential, abundant reduced inorganic compounds such as $H_2$
641 and $H_2S$ in this settings are also essential factors for nitrogen fixation by
642 chemolithoautotrophs, and they are derived from the anaerobic fermentation of
643 organic matter and sulfate reduction in sediments, respectively.
644 Potential chemolithoautotrophic diazotrophs may fill an essential ecological
645 niche, contributing to the initial accumulation of organic carbon and nitrogen in
646 mangrove sediments and facilitating ecosystem productivity, which is similar to their
647 roles in oligotrophic habitats such as tailings or glacier forefields[19,20]. A conceptual

model of depth and redox-related microbial nitrogen fixation by different energy sources was constructed (**Fig. 7**). In the upper 0-18 cm sediment layer (Eh = ~ -117 mV), chemolithoautotrophs are the most predominant and active diazotrophs, which utilize hydrogen, reduced sulfur species, and iron as the electron donors, with oxygen, nitrate, and sulfur as terminal electron acceptors. Moreover, carbon dioxide is used by these chemolithoautotrophs to form new organic carbon that feeds heterotrophs within the microbial assemblages. In the deeper sediments around 18-20 cm (Eh = -120 mV), diazotrophs involved in dissimilatory sulfate reduction and methanogenesis are strongly enriched. A large amount of sulfide is produced from sulfate-reducing bacteria via organic matter mineralization or $H_2$ oxidation, and then diffuses upward, where it is further utilized by chemolithoautotrophic sulfur-oxidizing bacteria in upper sediments to form thiosulfate and even sulfate. Small molecule compounds such as formate, acetate, propionate, butyrate, $H_2$, and $CO_2$ originate from the anaerobic fermentation of macromolecules in deeper layers of mangrove sediments[36].

## Conclusions

The findings from this research significantly enhance our understanding of biological nitrogen fixation within coastal eutrophic sediments, shedding light on the ecological significance of chemolithoautotrophic organisms in nitrogen metabolism. Our results showed that an unexpectedly diverse assemblage of chemolithoautotrophs including *Campylobacterota*, *Pseudomonadota*, and *Nitrospirota* are the predominant and active nitrogen fixers in the surface sediments of mangroves. They play a pivotal role in carbon and sulfur elemental cycling by mitigating nitrogen shortages in mangrove

sediments that are rich in carbon and sulfur. From a metabolic standpoint, reduced sulfur, hydrogen, and iron serve as the principal energy sources for microbial chemosynthesis. These chemolithoautotrophic diazotrophs are deemed crucial not only in mangrove sediments but also in other habitats where there is a disparity between carbon and nitrogen and a richness in reduced inorganic compounds. Future studies are needed to quantify the contribution of these chemolithoautotrophs to the total amount of nitrogen fixation *in situ*.

## Data availability

All metagenomic and metatranscriptomic raw reads used in this study are available in NCBI under accessions SAMN37418899-37418908 (BioProject PRJNA1017975) and SAMN37429165-37429174 (BioProject PRJNA1018229), respectively. The sequences from 16S rRNA gene and genome in ten strains are available in NCBI with the accession numbers shown in **Table S9**. The assemblies, reference gene catalog, all MAGs, and phylogenetic trees could be found in figshare (https://doi.org/10.6084/m9.figshare.24331438).

## References

1. Kuypers MMM, Marchant HK, Kartal B. The microbial nitrogen-cycling network. Nat Rev Microbiol. 2018;16:263-76.

2. Zehr JP, Capone DG. Changing perspectives in marine nitrogen fixation. Science. 2020;368:eaay9514.

3. Garcia AK, McShea H, Kolaczkowski B, Kaçar B. Reconstructing the evolutionary history of nitrogenases: evidence for ancestral molybdenum-cofactor utilization.

692 Geobiology. 2020;18:394-411.
693 4. Gruber N, Galloway JN. An Earth-system perspective of the global nitrogen cycle.
694 Nature. 2008;451:293-6.
695 5. Galloway JN, Dentener FJ, Capone DG, Boyer EW, Howarth RW, Seitzinger SP, et
696 al. Nitrogen cycles: past, present, and future. Biogeochemistry. 2004;70:153-226.
697 6. Karl D, Letelier R, Tupas L, Dore J, Christian J, Hebel D. The role of nitrogen
698 fixation in biogeochemical cycling in the subtropical North Pacific Ocean. Nature.
699 1997;388:533-8.
700 7. Mosley OE, Gios E, Close M, Weaver L, Daughney C, Handley KM. Nitrogen
701 cycling and microbial cooperation in the terrestrial subsurface. ISME J.
702 2022;16:2561-73.
703 8. Delmont TO, Pierella Karlusich JJ, Veseli I, Fuessel J, Eren AM, Foster RA, et al.
704 Heterotrophic bacterial diazotrophs are more abundant than their cyanobacterial
705 counterparts in metagenomes covering most of the sunlit ocean. ISME J.
706 2021;16:927-36.
707 9. Elser JJ, Bracken ME, Cleland EE, Gruner DS, Harpole WS, Hillebrand H, et al.
708 Global analysis of nitrogen and phosphorus limitation of primary producers in
709 freshwater, marine, and terrestrial ecosystems. Ecol Lett. 2007;10:1135-42.
710 10. Dong X, Zhang C, Peng Y, Zhang HX, Shi LD, Wei G, et al. Phylogenetically and
711 catabolically diverse diazotrophs reside in deep-sea cold seep sediments. Nat
712 Commun. 2022;13:4885.
713 11. Tian L, Yan Z, Wang C, Xu S, Jiang H. Habitat heterogeneity induces regional

differences in sediment nitrogen fixation in eutrophic freshwater lake. Sci Total Environ. 2021;772:145594.

12. Sohm JA, Webb EA, Capone DG. Emerging patterns of marine nitrogen fixation. Nat Rev Microbiol. 2011;9:499-508.

13. Mendez MO, Neilson JW, Maier RM. Characterization of a bacterial community in an abandoned semiarid lead-zinc mine tailing site. Appl Environ Microbiol. 2008; 74:3899-907.

14. Desai MS, Assig K, Dattagupta S. Nitrogen fixation in distinct microbial niches within a chemoautotrophy-driven cave ecosystem. ISME J. 2013;7:2411-23.

15. König S, Gros O, Heiden SE, Hinzke T, Thürmer A, Poehlein A, et al. Nitrogen fixation in a chemoautotrophic lucinid symbiosis. Nat Microbiol. 2016;2:16193.

16. Middelburg JJ, Mueller CE, Veuger B, Larsson AI, Form A, Van Oevelen D. Discovery of symbiotic nitrogen fixation and chemoautotrophy in cold-water corals. Sci Rep. 2015;5:17962.

17. Dekas AE, Poretsky RS, Orphan VJ. Deep-sea archaea fix and share nitrogen in methane-consuming microbial consortia. Science. 2009;326:422-6.

18. Mehta MP, Baross JA. Nitrogen fixation at 92 degrees C by a hydrothermal vent archaeon. Science. 2006;314:1783-6.

19. Sun X, Kong T, Häggblom MM, Kolton M, Li F, Dong Y, et al. Chemolithoautotropic diazotrophy dominates the nitrogen fixation process in mine tailings. Environ Sci Technol. 2020;54:6082-93.

20. Schmidt SK, Reed SC, Nemergut DR, Grandy AS, Cleveland CC, Weintraub MN,

et al. The earliest stages of ecosystem succession in high-elevation (5000 metres above sea level), recently deglaciated soils. Proc Biol Sci. 2008;275:2793-802.

21. Nelson DC, Waterbury JB, Jannasch HW. Nitrogen fixation and nitrate utilization by marine and freshwater *Beggiatoa*. Arch Microbiol. 1982;133:172-7.

22. Hou L, Wang R, Yin G, Liu M, Zheng Y. Nitrogen fixation in the intertidal sediments of the yangtze estuary: occurrence and environmental implications. J Geophys Res Biogeo. 2018;123:936-44.

23. Li S, Twilley RR, Hou A. Heterotrophic nitrogen fixation in response to nitrate loading and sediment organic matter in an emerging coastal deltaic floodplain within the Mississippi River Delta plain. Limnol Oceanogr. 2021;66:1961-78.

24. Newell SE, Pritchard KR, Foster SQ, Fulweiler RW. Molecular evidence for sediment nitrogen fixation in a temperate New England estuary. PeerJ. 2016;4:e1615.

25. Bertics VJ, Löscher CR, Salonen I, Dale AW, Gier J, Schmitz RA, et al. Occurrence of benthic microbial nitrogen fixation coupled to sulfate reduction in the seasonally hypoxic Eckernförde Bay, Baltic Sea. Biogeosciences. 2013;10:1243-58.

26. Fulweiler RW, Brown SM, Nixon SW, Jenkins BD. Evidence and a conceptual model for the co-occurrence of nitrogen fixation and denitrification in heterotrophic marine sediments. Mar Ecol Prog Ser. 2013;482:57-68.

27. Bird C, Martinez JM, O'Donnell AG, Wyman M. Spatial distribution and transcriptional activity of an uncultured clade of planktonic diazotrophic $\gamma$-proteobacteria in the Arabian sea. Appl Environ Microbiol. 2005;71:2079-85.

28. Sengupta A, Chaudhuri S. Ecology of heterotrophic dinitrogen fixation in the

rhizosphere of mangrove plant community at the Ganges river estuary in India. Oecologia.1991;87:560-4.

29. Duke NC, Meynecke JO, Dittmann S, Ellison AM, Anger K, Berger U, et al. A world without mangroves? Science. 2007;317:41-2.

30. Holguin G, Vazquez P, Bashan Y. The role of sediment microorganisms in the productivity, conservation and rehabilitation of the mangrove ecosystems: an overview. Biol Fertil Soils. 2001;33:265-78.

31. Andreote FD, Jiménez DJ, Chaves D, Dias ACF, Luvizotto DM, Dini-Andreote F, et al. The microbiome of Brazilian mangrove sediments as revealed by metagenomics. Plos ONE. 2012;7:e38600.

32. Inoue T, Shimono A, Akaji Y, Baba S, Takenaka A, Tuck CH. Mangrove-diazotroph relationships at the root, tree and forest scales: diazotrophic communities create high soil nitrogenase activities in *Rhizophora stylosa* rhizospheres. Ann Bot. 2019;125:131-44.

33. Jing H, Xia X, Liu H, Zhou Z, Wu C, Nagarajan S. Anthropogenic impact on diazotrophic diversity in the mangrove rhizosphere revealed by *nifH* pyrosequencing. Front Microbiol. 2015;6:1172.

34. Luo Z, Zhong Q, Han X, Hu R, Liu X, Xu W, et al. Depth-dependent variability of biological nitrogen fixation and diazotrophic communities in mangrove sediments. Microbiome. 2021;9:212.

35. Zhang Y, Yang Q, Ling J, Van Nostrand JD, Shi Z, Zhou J, et al. Diversity and structure of diazotrophic communities in mangrove rhizosphere, revealed by high-

780 throughput sequencing. Front Microbiol. 2017;8:2032.
781 36. Lin X, Hetharua B, Lin L, Xu H, Zheng T, He Z, et al. Mangrove sediment
782 microbiome: adaptive microbial assemblages and their routed biogeochemical
783 processes in Yunxiao Mangrove National Nature Reserve. China Microb Ecol.
784 2019;78:57-69.
785 37. Qian L, Yu X, Gu H, Liu F, Fan Y, Wang C, et al. Vertically stratified methane,
786 nitrogen and sulfur cycling and coupling mechanisms in mangrove sediment
787 microbiomes. Microbiome. 2023;11:71.
788 38. Gong B, Cao H, Peng C, Perčulija V, Tong G, Fang H, et al. High-throughput
789 sequencing and analysis of microbial communities in the mangrove swamps along the
790 coast of Beibu Gulf in Guangxi, China. Sci Rep. 2019;9:9377.
791 39. Behera B, Mishra R, Dutta S, Thatoi H. Sulfur oxidizing bacteria in mangrove
792 ecosystem: a review. Afr J Biotechnol. 2014;13:2897-907.
793 40. Vandieken V, Finke N, Thamdrup B. Hydrogen, acetate, and lactate as electron
794 donors for microbial manganese reduction in a manganese-rich coastal marine
795 sediment. FEMS Microbiol Ecol. 2014;87:733-45.
796 41. Hettiarachchi SR, Maher WA, Krikowa F, Ubrihien R. Factors influencing arsenic
797 concentrations and species in mangrove surface sediments from south-east NSW,
798 Australia. Environ Geochem Health. 2017;39:209-19.
799 42. Chowdhury N, Marschner P, Burns R. Response of microbial activity and
800 community structure to decreasing soil osmotic and matric potential. Plant Soil. 2011;
801 344:241-54.

802 43. Sims GK, Ellsworth TR, Mulvaney RL, Microscale determination of inorganic
803 nitrogen in water and soil extracts. Commun Soil Sci Plan.1995;26:303-16.
804 44. Hsieh YP, Shieh YN. Analysis of reduced inorganic sulfur by diffusion methods:
805 improved apparatus and evaluation for sulfur isotopic studies. Chem Geol.
806 1997;137:255-61.
807 45. Yu X, Yang X, Wu Y, Peng Y, Yang T, Xiao F. *Sonneratia apetala* introduction
808 alters methane cycling microbial communities and increases methane emissions in
809 mangrove ecosystems. Soil Boil Biochem. 2020;144:107775.
810 46. Bartram AK, Lynch MD, Stearns JC, Moreno-Hagelsieb G, Neufeld JD.
811 Generation of multimillion-sequence 16S rRNA gene libraries from complex
812 microbial communities by assembling paired-end Illumina reads. Appl Environ
813 Microbiol. 2011;77:3846-52.
814 47. Chen S, Zhou Y, Chen Y, Gu J. fastp: an ultra-fast all-in-one FASTQ preprocessor.
815 Bioinformatics. 2018;34:i884-90.
816 48. Mago T, Salzberg SL. Flash: fast length adjustment of short reads to improve
817 genome assemblies. Bioinformatics. 2011;27:2957-63.
818 49. Callahan BJ, Mcmurdie PJ, Rosen MJ, Han AW, Johnson AJA, Holmes SP.
819 DADA2: high-resolution sample inference from Illumina amplicon data. Nat
820 Methods. 2016;13:581-3.
821 50. Bolyen E, Rideout JR, Dillon MR, Bokulich NA, Abnet CC, Al-Ghalith GA, et al.
822 Reproducible, interactive, scalable and extensible microbiome data science using
823 QIIME 2. Nat Biotechnol. 2019;37:852-7.

824 51. Henderson G, Yilmaz P, Kumar S, Forster RJ, Kelly WJ, Leahy SC, et al.
825 Improved taxonomic assignment of rumen bacterial 16S rRNA sequences using a
826 revised SILVA taxonomic framework. PeerJ. 2019;7:e6496.
827 52. Zhou Z, Meng H, Liu Y, Gu JD, Li M. Stratified bacterial and archaeal community
828 in mangrove and intertidal wetland mudflats revealed by high throughput 16S rRNA
829 gene sequencing. Front Microbiol. 2017;8:2148.
830 53. Li D, Liu CM, Luo R, Sadakane K, Lam TW. MEGAHIT: an ultra-fast single-
831 node solution for large and complex metagenomics assembly via succinct de Bruijn
832 graph. Bioinformatics. 2015;31:1674-6.
833 54. Hyatt D, Chen GL, Locascio PF, Land ML, Larimer FW, Hauser LJ. Prodigal:
834 prokaryotic gene recognition and translation initiation site identifcation. BMC
835 Bioinformatics. 2010;11:119.
836 55. Fu L, Niu B. Zhu Z, Wu S, Li W. CD-HIT: accelerated for clustering the next-
837 generation sequencing data. Bioinformatics. 2012;28:3150-2.
838 56. Uritskiy GV, DiRuggiero J, Taylor J. MetaWRAP-a flexible pipeline for genome-
839 resolved metagenomic data analysis. Microbiome. 2018;6:158.
840 57. Nissen JN, Johansen J, Allesøe RL, Sønderby CK, Armenteros JJA, Grønbech
841 CH, et al. Improved metagenome binning and assembly using deep variational
842 autoencoders. Nat Biotechnol. 2021;39:555-60.
843 58. Olm MR, Brown CT, Brooks B. Banfeld JF. dRep: a tool for fast and accurate
844 genomic comparisons that enables improved genome recovery from metagenomes
845 through de-replication. ISME J. 2017;11:2864-8.

59. Parks DH, Imelfort M, Skennerton CT, Hugenholtz P, Tyson GW. CheckM: assessing the quality of microbial genomes recovered from isolates, single cells, and metagenomes. Genome Res. 2015;25:1043-55.

60. Orakov A, Fullam A, Coelho LP, Khedkar S, Szklarczyk D, Mende DR, et al. GUNC: detection of chimerism and contamination in prokaryotic genomes. Genome Biol. 2021;22:178.

61. Nayfach S, Shi ZJ, Seshadri R, Pollard KS, Kyrpides NC. New insights from uncultivated genomes of the global human gut microbiome. Nature. 2019;568: 505-10.

62. Parks DH, Chuvochina M, Rinke C, Mussig AJ, Chaumeil PA, Hugenholtz P. GTDB: an ongoing census of bacterial and archaeal diversity through a phylogenetically consistent, rank normalized and complete genome-based taxonomy. Nucleic Acids Res. 2022;50:D785-94.

63. Nguyen LT, Schmidt HA, von Haeseler A, Minh BQ. IQ-TREE: A fast and effective stochastic algorithm for estimating maximum-likelihood phylogenies. Mol Biol Evol. 2015;32:268-74.

64. Letunic I, Bork P. Interactive Tree Of Life (iTOL) v5: an online tool for phylogenetic tree display and annotation. Nucleic Acids Res. 2021;49:W293-6.

65. Buchfink B, Xie C, Huson DH. Fast and sensitive protein alignment using DIAMOND. Nat Methods. 2014;12:59.

66. Chen YJ, Leung PM, Wood JL, Bay SK, Hugenholtz P, Kessler AJ, et al. Metabolic flexibility allows bacterial habitat generalists to become dominant in a

frequently disturbed ecosystem. ISME J. 2021;15:2986-3004.

67. Greening C, Geier R, Wang C, Woods LC, Morales SE, McDonald MJ, et al. Diverse hydrogen production and consumption pathways influence methane production in ruminants. ISME J. 2019;13:2617-32.

68. Kanehisa M, Sato Y, Kawashima M, Furumichi M, Tanabe M. KEGG as a reference resource for gene and protein annotation. Nucleic Acids Res. 2016;44:D457-62.

69. Graham ED, Heidelberg JF, Tully BJ. Potential for primary productivity in a globally-distributed bacterial phototroph. ISME J. 2018;12:1861-6.

70. Zhou Z, Tran PQ, Breister AM, Liu Y, Kieft K, Cowley ES, et al. METABOLIC: high-throughput profling of microbial genomes for functional traits, metabolism, biogeochemistry, and community-scale functional networks. Microbiome. 2022;10:33.

71. Aziz RK, Bartels D, Best AA, DeJongh M, Disz T, Edwards RA, et al. The RAST Server: rapid annotations using subsystems technology. BMC Genomics. 2008;9:75.

72. Katoh K, Standley DM. A simple method to control overalignment in the MAFFT multiple sequence alignment program. Bioinformatics. 2016;32:1933-42.

73. Capella-Gutierrez S, Silla-Martinez JM, Gabaldon T. trimAl: a tool for automated alignment trimming in large-scale phylogenetic analyses. Bioinformatics. 2009;25:1972-3.

74. Madeira F, Park YM, Lee J, Buso N, Gur T, Madhusoodanan N, et al. The EMBL-EBI search and sequence analysis tools APIs in 2019. Nucleic Acids Res.

2019;47:W636-41.

75. Waterhouse AM, Procter JB, Martin DM, Clamp M, Barton GJ. Jalview version 2-a multiple sequence alignment editor and analysis workbench. Bioinformatics. 2009;25:1189-91.

76. Patro R, Duggal G, Love MI, Irizarry RA, Kingsford C. Salmon provides fast and bias-aware quantifcation of transcript expression. Nat Methods. 2017;14:417-9.

77. Zhang C, Fang YX, Yin X, Lai H, Kuang Z, Zhang T, et al. The majority of microorganisms in gas hydrate-bearing subseafloor sediments ferment macromolecules. Microbiome. 2023;11:37.

78. Zhang C, Liu X, Shi LD, Li J, Xiao X, Shao Z, et al. Unexpected genetic and microbial diversity for arsenic cycling in deep sea cold seep sediments. NPJ Biofilms Microbi. 2023;9:13.

79. Han Y, Zhang C, Zhao Z, Peng Y, Liao J, Jiang Q, et al. A comprehensive genomic catalog from global cold seeps. Sci Data. 2023;10:596.

80. Kopylova E, Noe L, Touzet H. SortMeRNA: fast and accurate fltering of ribosomal RNAs in metatranscriptomic data. Bioinformatics. 2012;28:3211-7.

81. Takai K, Inagaki F, Nakagawa S, Hirayama H, Nunoura T, SakoY, et al. Isolation and phylogenetic diversity of members of previously uncultivated ε-Proteobacteria in deep-sea hydrothermal fields. FEMS Microbiol Lett. 2003;218:167-74.

82. Jiang L, Zheng Y, Peng X, Zhou H, Zhang C, Xiao X, et al. Vertical distribution and diversity of sulfate-reducing prokaryotes in the Pearl River estuarine sediments, Southern China. FEMS Microbiol Ecol. 2009;70:93-106.

912 83. Wang S, Shao Z, Lai Q, Liu X, Xie S, Jiang L, et al. *Sulfurimonas sediminis* sp.
913 nov., a novel hydrogen- and sulfur-oxidizing chemolithoautotroph isolated from a
914 hydrothermal vent at the Longqi system, southwestern Indian ocean. Antonie Van
915 Leeuwenhoek. 2021;114:813-22.
916 84. Liu X, Li P, Wang H, Han LL, Yang K, Wang Y, et al. Nitrogen fixation and
917 diazotroph diversity in groundwater systems. ISME J. 2023;17:2023-34.
918 85. Li Y, Guo L, Häggblom MM, Yang R, Li M, Sun X, et al. *Serratia* spp. are
919 responsible for nitrogen fixation fueled by As(III) oxidation, a novel biogeochemical
920 process identified in mine tailings. Environ Sci Technol. 2022;56:2033-43.
921 86. Zheng H, Dietrich C, Radek R, Brune A. *Endomicrobium proavitum*, the first
922 isolate of *Endomicrobia* class. nov. (phylum *Elusimicrobia*)-an ultramicrobacterium
923 with an unusual cell cycle that fixes nitrogen with a Group IV nitrogenase. Environ
924 Microbiol. 2016;18:191-204.
925 87. Liesirova T, Launbjerg TA, Hallstrøm S, Bittner MJ, Riemann L, Voss M.
926 Nitrogen-fixing sulfate reducing bacteria in shallow coastal sediments under
927 simulated resuspension. Estuar Coast Shelf S. 2023;280:108165.
928 88. Khan NS, Vane CH, Engelhart SE, Kendrick C, Horton BP. The application of
929 $\delta^{13}C$, TOC and C/N geochemistry of mangrove sediments to reconstruct Holocene
930 paleoenvironments and relative sea levels, Puerto Rico. Mar Geol. 2019;415:105963.
931 89. Zhang CJ, Liu YR, Cha G, Liu Y, Zhou XQ, Lu Z, et al. Potential for mercury
932 methylation by Asgard archaea in mangrove sediments. ISME J. 2023;17:478-85.
933 90. Kapili BJ, Barnett SE, Buckley DH, Dekas AE. Evidence for phylogenetically and

catabolically diverse active diazotrophs in deep-sea sediment. ISME J. 2020; 14:971-83.

91. Moisander PH, Serros T, Paerl RW, Beinart RA, Zehr JP. Gammaproteobacterial diazotrophs and *nifH* gene expression in surface waters of the South Pacific Ocean. ISME J. 2014;8:1962-73.

92. North JA, Narrowe AB, Xiong W, Byerly KM, Zhao G, Young SJ, et al. A nitrogenase-like enzyme system catalyzes methionine, ethylene, and methane biogenesis. Science. 2020;369:1094-8.

93. Raymond J, Siefert JL, Staples CR, Blankenship RE. The natural history of nitrogen fixation. Mol Biol Evol. 2004;21:541-54.

94. Boyd ES, Hamilton TL. Peters JW. An alternative path forthe evolution of biological nitrogen fixation. Front Microbiol. 2011;2:205.

95. Koirala A. Brozel VS. Phylogeny of nitrogenase structural and assembly components reveals new insights into the origin and distribution of nitrogen fixation across bacteria and archaea. Microorganisms. 2021;9:1662.

96. Rogers TJ, Buongiorno J, Jessen GL, Schrenk MO, Fordyce JA, de Moor JM, et al. Chemolithoautotroph distributions across the subsurface of a convergent margin. ISME J. 2023;17:140-50.

97. McAllister SM, Moore RM, Gartman A, Luther GW, Emerson D, Chan CS. The Fe(II)-oxidizing *Zetaproteobacteria*: historical, ecological and genomic perspectives. FEMS Microbiol Ecol. 2019;95:fiz015.

98. Fernández-Gómez B, Richter M, Schüler M, Pinhassi J, Acinas SG, González JM,

et al. Ecology of marine *Bacteroidetes*: a comparative genomics approach. ISME J. 2013;7:1026-37.

99. Fuerst JA, Sagulenko E. Beyond the bacterium: planctomycetes challenge our concepts of microbial structure and function. Nat Rev Microbiol. 2011;9:403-13.

100. Campbell BJ, Engel AS, Porter ML, Takai K. The versatile ε-proteobacteria: key players in sulfidic habitats. Nat Rev Microbiol. 2006;4:458-68.

101. Waite DW, Vanwonterghem I, Rinke C, Parks DH, Zhang Y, Takai K, et al. Comparative genomic analysis of the class *Epsilonproteobacteria* and proposed reclassification to *Epsilonbacteraeota* (phyl. nov.). Front Microbiol. 2017;8:682.

102. Adam N, Perner M. Microbially mediated hydrogen cycling in deep-sea hydrothermal vents. Front Microbiol. 2018;9:2873.

103. Fang Y, Liu J, Yang J, Wu G, Hua Z, Dong H, et al. Compositional and metabolic responses of autotrophic microbial community to salinity in lacustrine environments. mSystems. 2022;7:e0033522.

104. Bueno E, Mesa S, Bedmar EJ, Richardson DJ, Delgado MJ. Bacterial adaptation of respiration from oxic to microoxic and anoxic conditions: redox control. Antioxid Redox Signal. 2012;16:819-52.

105. Grote J, Schott T, Bruckner CG, Glockner FO, Jost G, Teeling H, et al. Genome and physiology of a model *Epsilonproteobacterium* responsible for sulfide detoxification in marine oxygen depletion zones. Proc Natl Acad Sci USA. 2012;109:506-10.

106. Bell E, Lamminmäki T, Alneberg J, Andersson AF, Qian C, Xiong W, et al.

978 Active sulfur cycling in the terrestrial deep subsurface. ISME J. 2020;14:1260-72.
979 107. Frank YA, Kadnikov VV, Lukina AP, Banks D, Beletsky AV, Mardanov AV, et al.
980 Characterization and genome analysis of the first facultatively alkaliphilic
981 *Thermodesulfovibrio* isolated from the deep terrestrial subsurface. Front Microbiol.
982 2016;7:2000.
983 108. Bhatnagar S, Badger JH, Madupu R, Khouri HM, O'Connor EM, Robb FT, et al.
984 Genome sequence of the sulfate-reducing thermophilic bacterium
985 *Thermodesulfovibrio yellowstonii* Strain DSM 11347$^{T}$ (Phylum *Nitrospirae*). Genome
986 Announc. 2015;3:e01489-14.
987 109. Medlar AJ, Törönen P, Holm L. AAI-profiler: fast proteome-wide exploratory
988 analysis reveals taxonomic identity, misclassiffcation and contamination. Nucleic
989 Acids Res. 2018;46:W479-85.
990 110. Na SI, Kim YO, Yoon SH, Ha SM, Baek I, Chun J. UBCG: Up-to-date bacterial
991 core gene set and pipeline for phylogenomic tree reconstruction. J Microbiol.
992 2018;56:280-5.
993 111. Zehr JP, Jenkins BD, Short SM, Steward GF. Nitrogenase gene diversity and
994 microbial community structure: a cross-system comparison. Environ Microbiol.
995 2003;5:539-54.
996 112. Handley KM, Bartels D, O'Loughlin EJ, Williams KH, Trimble WL, Skinner K,
997 et al. The complete genome sequence for putative $H_2$- and S-oxidizer Candidatus
998 *Sulfuricurvum* sp., assembled de novo from an aquifer-derived metagenome. Environ
999 Microbiol. 2014;16:3443-62.

113. Yousuf J, Thajudeen J, Aneesa PA, Joseph A, Divya PS, Varghese A, et al. Diversity and activity of culturable nitrogen fixing heterotrophic bacteria from estuarine and coastal environments of Southeastern Arabian Sea (SEAS). Reg Stud Mar Sci. 2019;33:100973.

114. Dai C, Li J, Yan H, Lin W, Luo J. *Halothiobacillus diazotrophicus* sp. nov., a chemolithoautotrophic sulfur-oxidizing and nitrogen-fixing bacterium isolated from freshwater. Int J Syst Evol Microbiol. 2023;73:006202.

115. Bazylinski DA, Morillo V, Lefèvre CT, Viloria N, Dubbels BL, Williams TJ. *Endothiovibrio diazotrophicus* gen. nov., sp. nov., a novel nitrogen-fixing, sulfur-oxidizing gammaproteobacterium isolated from a salt marsh. Int J Syst Evol Microbiol. 2017;67:1491-8.

116. Nishihara A, Matsuura K, Tank M, McGlynn SE, Thiel V, Haruta S. Nitrogenase activity in thermophilic chemolithoautotrophic bacteria in the phylum *Aquificae* isolated under nitrogen-fixing conditions from Nakabusa Hot Springs. Microbes Environ. 2018;33:394-401.

117. Norris PR, Murrell JC, Hinson D. The potential for diazotrophy in iron-and sulfur-oxidizing acidophilic bacteria. Arch Microbiol. 1995;164:294-300.

118. Bothe H, Schmitz O, Yates MG, Newton WE. Nitrogen fixation and hydrogen metabolism in cyanobacteria. Microbiol Mol Biol Rev. 2010;74:529-51.

119. Greening C, Biswas A, Carere CR, Jackson CJ, Taylor MC, Stott MB, et al. Genomic and metagenomic surveys of hydrogenase distribution indicate $H_2$ is a widely utilised energy source for microbial growth and survival. ISME J. 2016;10:

761-77.

120. Hoffman BM, Lukoyanov D, Yang ZY, Dean DR, Seefeldt LC. Mechanism of nitrogen fixation by nitrogenase: the next stage. Chem Rev. 2014;114:4041-62.

121. Sievert SM, Scott KM, Klotz MG, Chain PSG, Hauser LJ, Hemp J, et al. Genome of the epsilonproteobacterial chemolithoautotroph *Sulfurimonas denitrificans*. Appl Environ Microbiol. 2008;74:1145-56.

122. Molari M, Hassenrueck C, Laso-Pérez R, Wegener G, Offre P, Scilipoti S, et al. A hydrogenotrophic *Sulfurimonas* is globally abundant in deep-sea oxygen-saturated hydrothermal plumes. Nat Microbiol. 2023;8:651-65.

123. Song JM, Li Y, Zhu ZB. Relationship between Eh value and Redox environment in marine sediments. B Mar Sci. 1990;9:33-9.

124. Nabuyanda MM, Kelderman P, Sankura MG, Rousseau D, Irvine K. Investigating the effect of Eh and pH on binding forms of Co, Cu, and Pb in wetland sediments from Zambia. J Environ Manage. 2022;319:115543.

125. Wang F, Chen N, Yan J, Lin J, Guo W, Cheng P, et al. Major processes shaping mangroves as inorganic nitrogen sources or sinks: insights from a multidisciplinary study. J Geophys Res. 2019;124:1194-208.

126. Fusi M, Booth JM, Marasco R, Merlino G, Garcias-Bonet N, Barozzi A, et al. Bioturbation intensity modifies the sediment microbiome and biochemistry and supports plant growth in an arid mangrove system. Microbiol Spectr. 2022; 10:e0111722.

## Acknowledgements

This work was financially supported by the National Natural Science Foundation of China (No. 42176134, 42306127 and 42030412), COMRA program (No. DY-XZ-04 and DY135-B2-01) and Scientific Research Foundation of Third Institute of Oceanography (No. 2019021; 2024002). We thank Prof. Fanghua Liu, Prof. Weimin Sun and their lab colleagues from institute of Eco-environmental and Soil Sciences, Guangdong Academy of Sciences for their support on the activity measurements by acetylene reduction assay.

## Author contributions

Z.S., and L.J. conceived this study. S.W., and L.J. designed the experiments. S.W., J.W., Y.Z., L.C., and Q.L. collected samples. S.W., Z.C., and J.W. carried out the geochemical analysis; Z.Z., and S.W. performed the omics analysis. S.W., Z.Z., Z.C., K.A., L.C., Y.P., X.D., L.J., and Z.S. interpreted the data. S.W., Z.C., and L.C. performed strain isolation and measurements of nitrogen fixation activities. S.W., X.D., L.J., and Z.S. wrote the paper, with input from other authors, and finally reviewed by X.D., L.J., and Z.S.

## Conflict of interest

The authors declare no conflict of interest.

## Figure legends

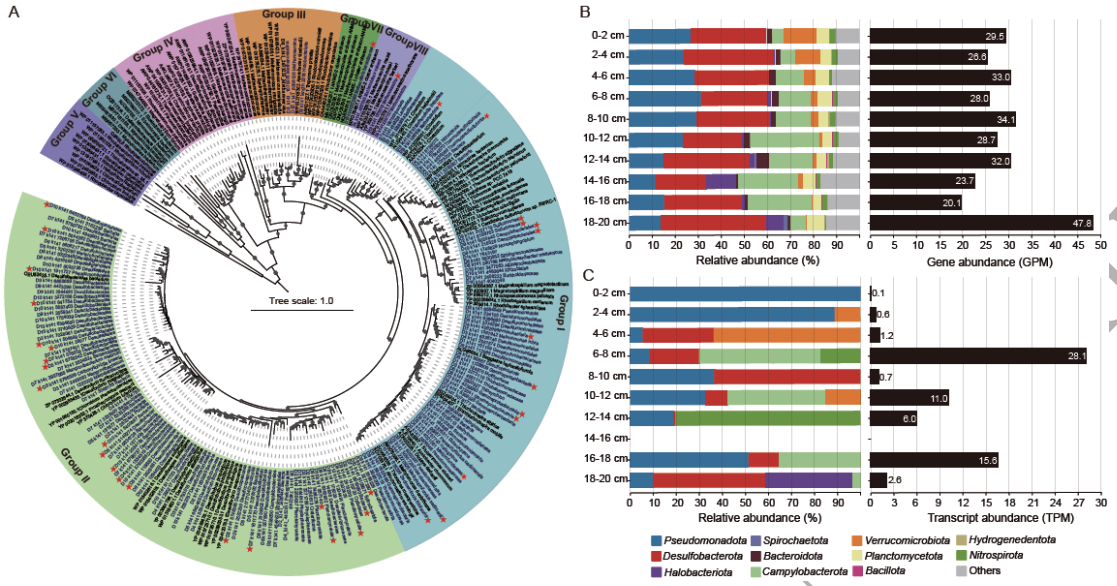


**Fig. 1. Summary of 154 non-redundant homologs of the nitrogenase subunit NifH from mangrove sediments.** A, Maximum-likelihood phylogenetic tree of NifH amino acid sequences. *nifH* homologs were classified into canonical groups I to III, nitrogen fixation-like groups IV to VI, and newly assigned groups VII and VIII. The NifH sequences obtained in this study are highlighted in blue, and sequences from diazotrophic MAGs are marked by stars. The scale bar indicates the mean number of substitutions per site. B, Relative abundances of *nifH* genes affiliated with different taxonomic groups (left) and the total values of gene abundance (right) in different mangrove sediment samples. C, Relative transcript abundances of *nifH* genes affiliated with different taxonomic groups (left) and the total values of transcript expression (right) in different sediment samples. Different taxonomic groups are represented by different colors. The "others" category represents unassigned sequences.

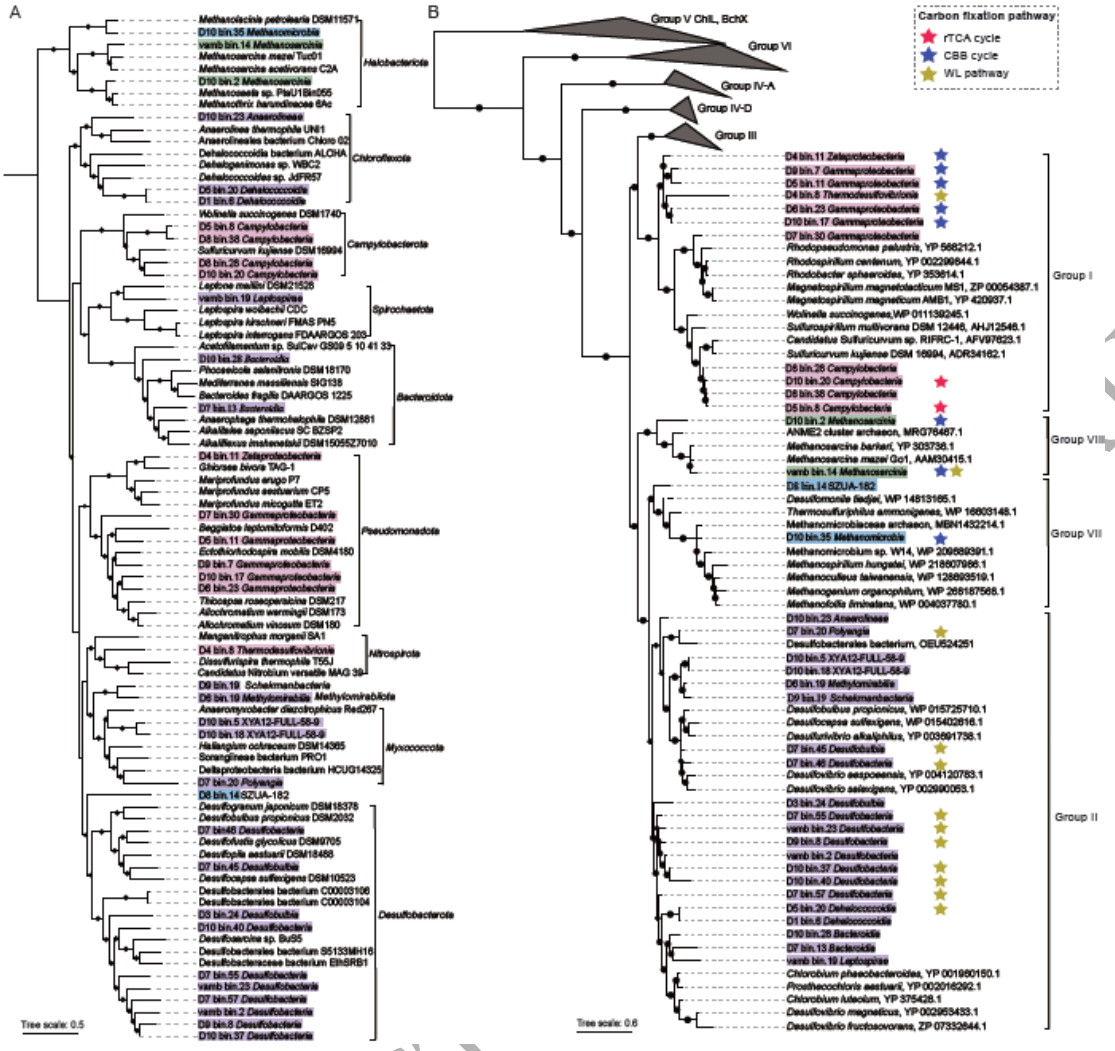


1077

1078 **Fig. 2. Phylogenetic trees of nitrogen-fixing MAGs and their NifH protein**
1079 **sequences.** A, Maximum-likelihood phylogenetic tree of 36 MAGs containing
1080 nitrogen fixation genes based on the concatenation of 43 conserved protein sequences.
1081 MAGs are color-coded according to their NifH homolog groups at the phylum level.
1082 B, Maximum-likelihood phylogenetic tree of identified NifH protein sequences within
1083 36 MAGs. Stars of different colors indicate different carbon fixation pathways, with
1084 red for rTCA, blue for CBB, and yellow for WL. For both trees, bootstrap values
1085 greater than 50% are denoted at the nodes, and scale bars represent the average
1086 number of substitutions per site.

1087

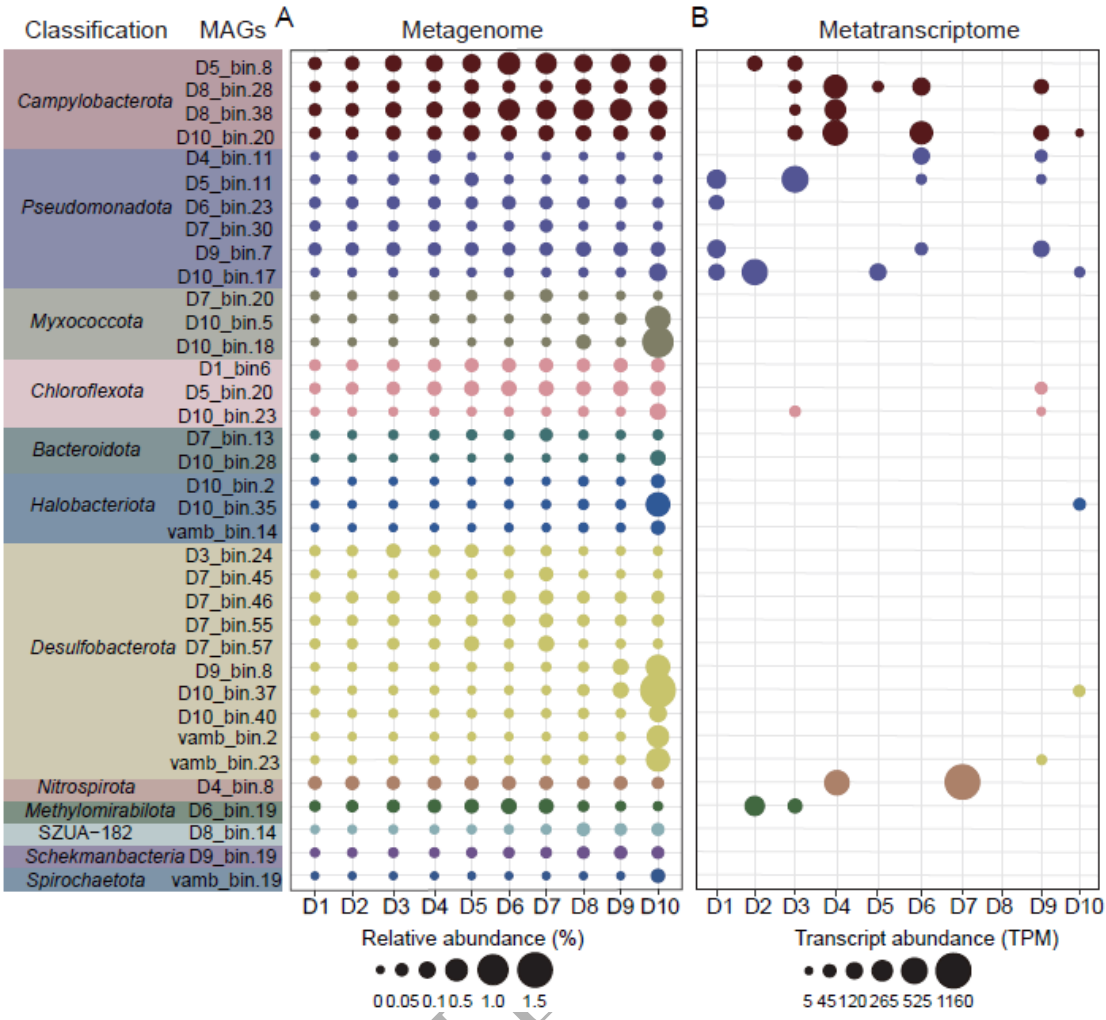


1088

1089 **Fig. 3. Relative abundance and expression of transcripts for 36 nitrogen-fixing**
1090 **MAGs at different mangrove sediment depths.** A, The relative abundance of each
1091 MAG was estimated using CoverM. B, The expression of transcripts for each MAG is
1092 represented in units of transcripts per million (TPM). The detailed information is
1093 given in Table S4 and Table S5.

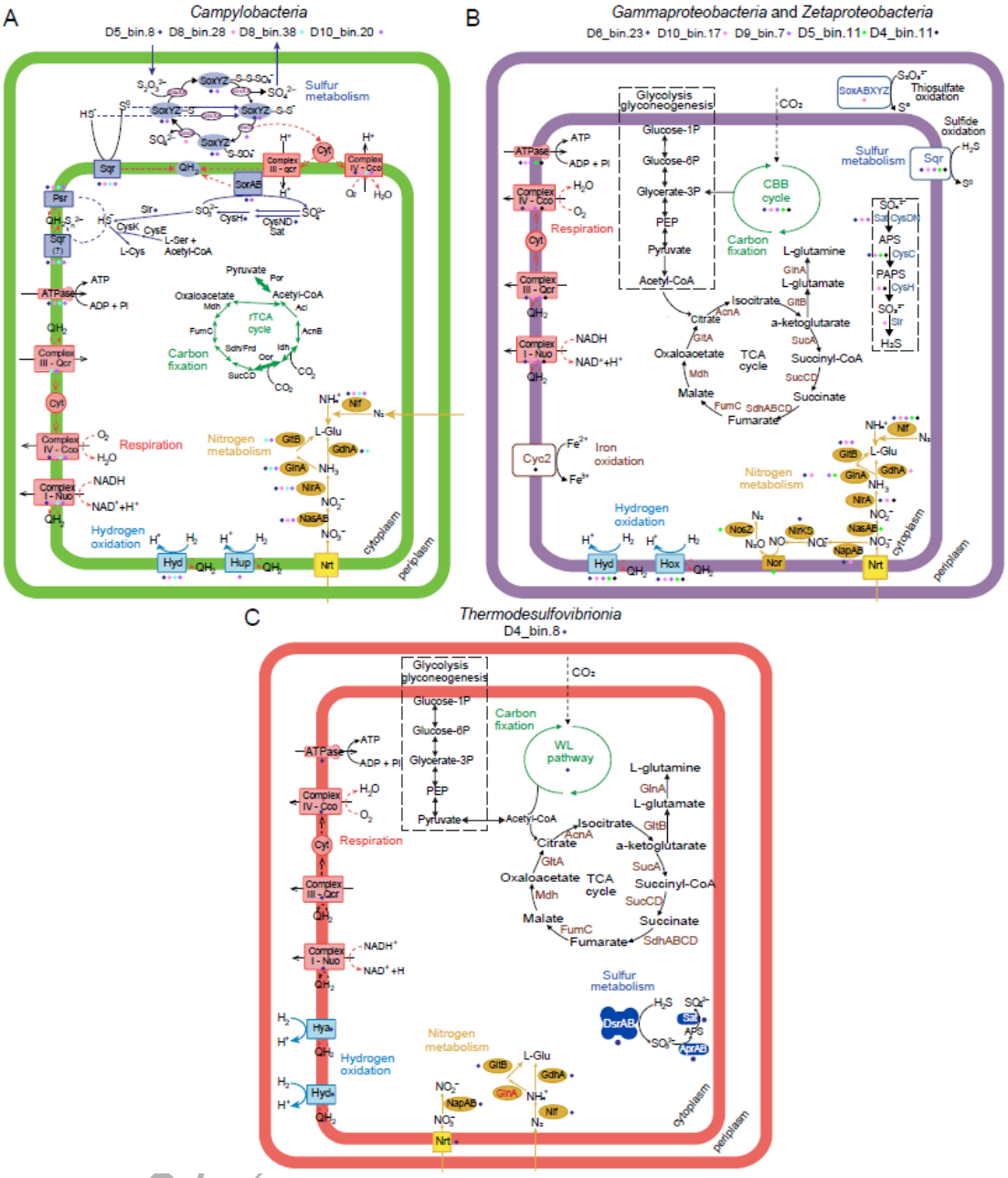


**Fig. 4. Metabolic pathway reconstructions for MAGs of dominant nitrogen-fixing chemolithoautotrophs.** Metabolic pathways are inferred for *Campylobacterota* (A), *Pseudomonadota* (B), and *Nitrospirota* (C), with the carbon fixation pathways of rTCA, CBB, and WL, respectively. Steps with more than one arrow indicate that several operons encoding different enzymes and catalyzing that reaction are present in the genome. Enzymes that are absent within these reconstructions are highlighted in red. Comprehensive enzyme annotations are provided in Tables S6-S8.

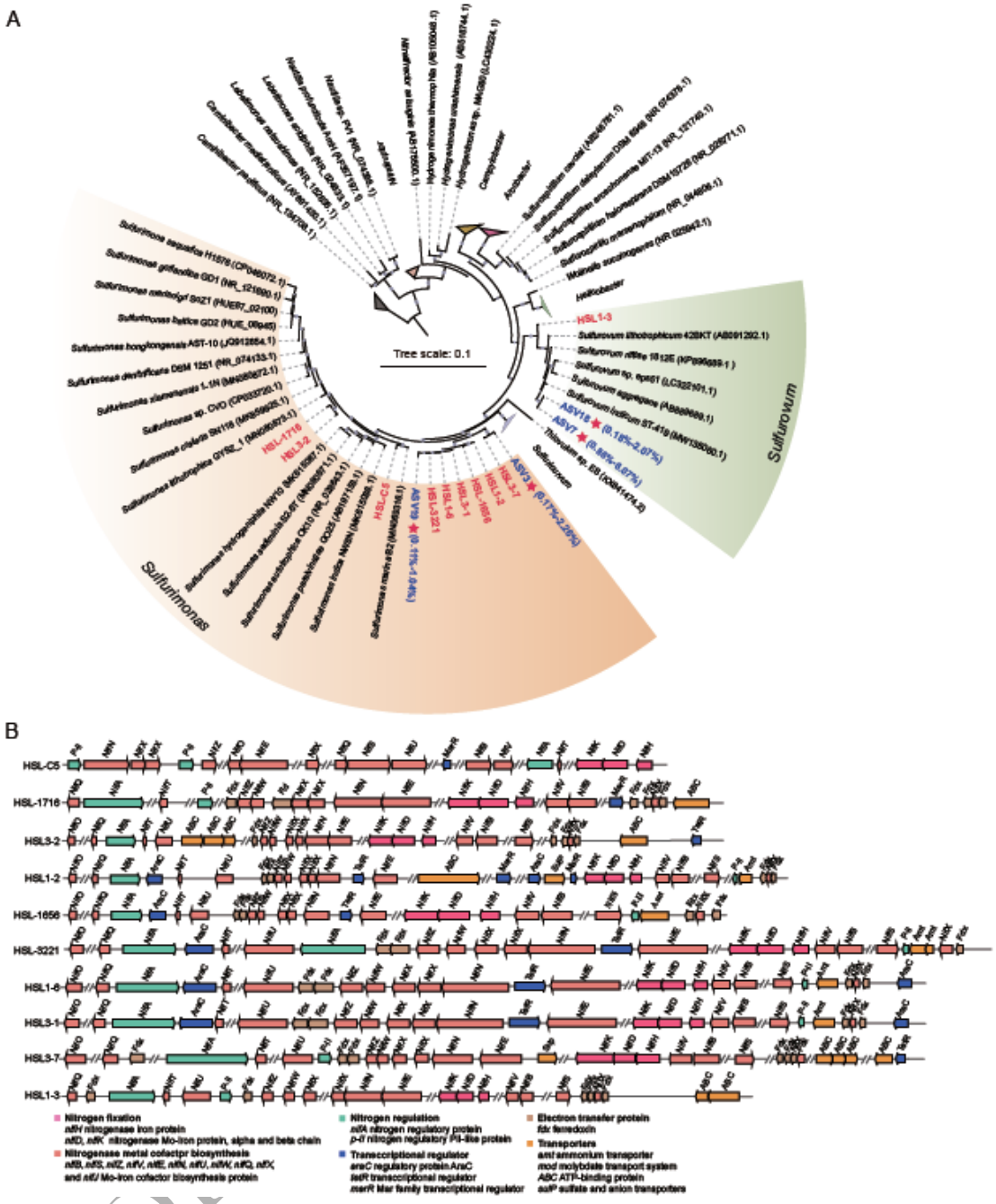


**Fig. 5. Phylogenetic analysis and nitrogen fixation gene clusters of ten isolates from *Campylobacterota*.** A, Phylogenetic tree based on 16S rRNA gene sequences from the representative ASVs of the genera *Sulfurimonas* and *Sulfurovum* and the isolates in this study. Only ASVs representing > 1% of the communities in at least one sample are shown. The scale bar represents 1.0 nucleotide replacements per site. B, Gene neighborhoods of *nifHDK* include nitrogenase metal cofactor biosynthesis genes, regulatory nitrogen fixation genes, transcriptional regulator genes, electron transfer genes and transporter genes.

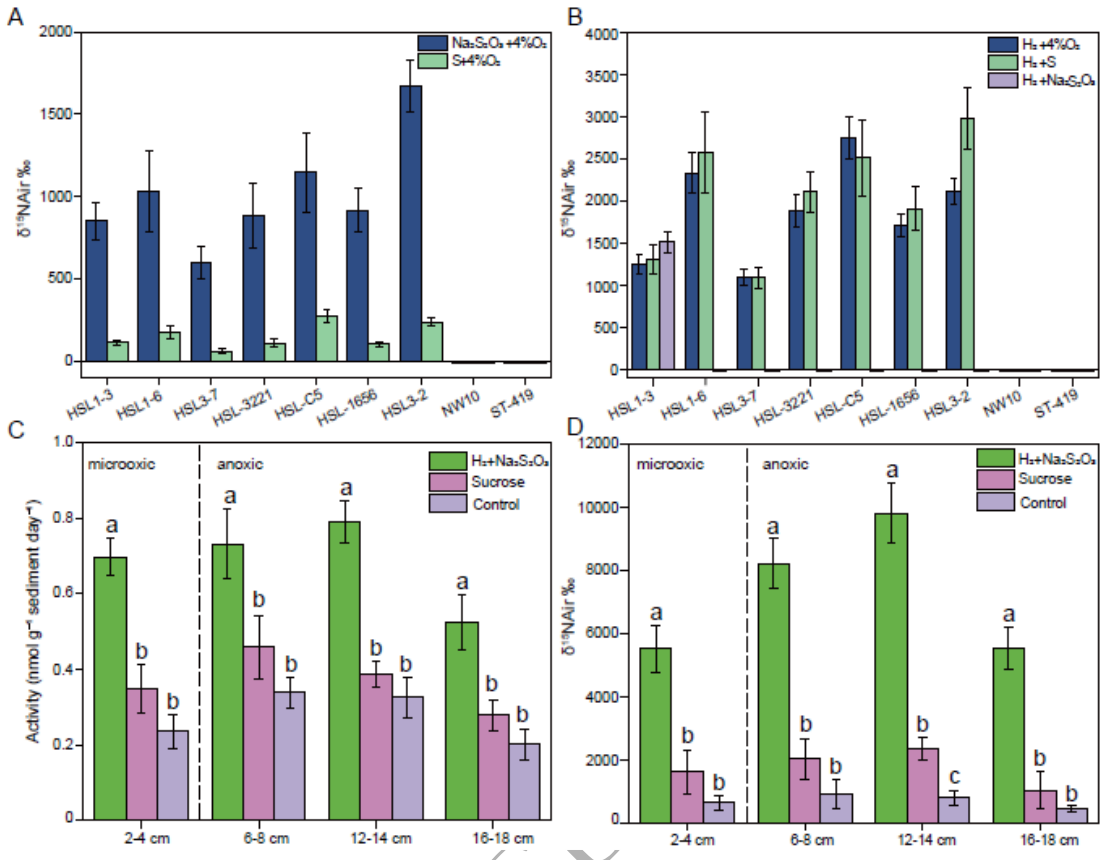


**Fig. 6. Nitrogen fixation activities in *Campylobacterota* representative strains and mangrove sediments.** A, $^{15}N$ abundance based on the $^{15}N_2$ incorporation assay for seven *Campylobacterota* strains incubated with different reduced sulfur compounds as the energy source. B, $^{15}N$ abundance based on the $^{15}N_2$ incorporation assay for seven *Campylobacterota* strains incubated with $H_2$ as the sole energy source coupled with different electron acceptors. The related type strains lacking the *nif* gene cluster are used as controls. C, Acetylene reduction assay of nitrogenase activity in four sediment layers incubated under chemolithoautotrophic and heterotrophic conditions. D, $^{15}N$ abundance based on the $^{15}N_2$ incorporation assay for four sediments incubated under chemolithoautotrophic and heterotrophic conditions. Standard deviations are indicated by error bars. The letters above the columns indicate statistically significant differences by Student's *t*-test ($P < 0.05$).

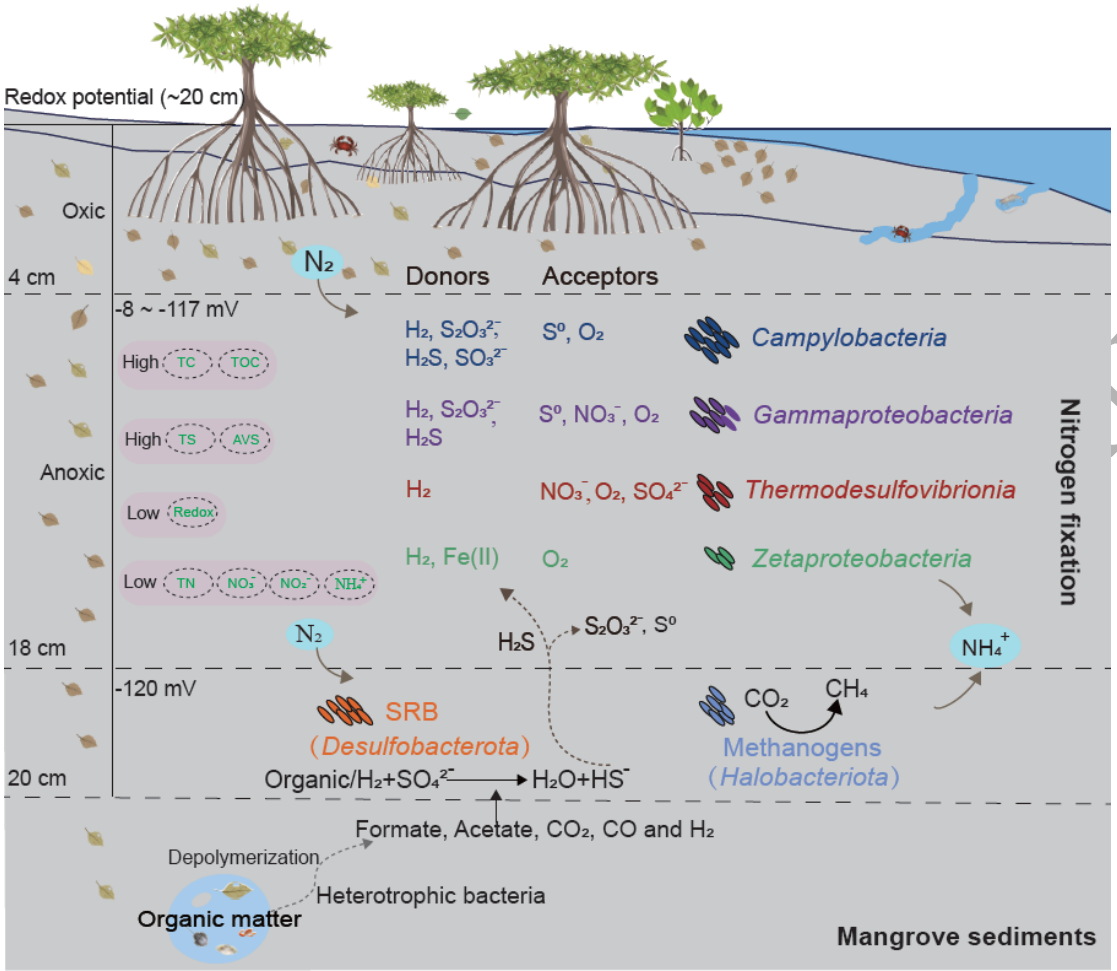


**Fig. 7. Conceptual model of depth-related microbial nitrogen fixation in mangrove sediments.** Upper sediments (0-18 cm): The model highlights the significance of chemolithoautotrophy, a previously overlooked energy source driving dark nitrogen fixation. These chemolithoautotrophic diazotrophs utilize inorganic compounds such as hydrogen, reduced sulfur, and iron as energy sources, with oxygen, nitrate, and sulfur as terminal electron acceptors. $H_2$ and $H_2S$ are produced by the degradation of organic matter and sulfate reduction, respectively. Deeper sediments (18-20 cm): The diazotrophs involved in dissimilatory sulfate reduction and methanogenesis are strongly enriched. Sulfate reduction is carried out utilizing the small molecule compounds produced from deeper sediments and resulting in abundant sulfide production.